DAFTAR PUSTAKA

Ahmed A., Murtaza M. A., 2016, CFD Analysis of car body aerodynamics including Effect of passive flow devices – a review, International Journal of Research in Engineering and Technology Volume: 05 Issue: 03 | Mar-2016.

Bruneau C. H., Creusé E., et al, 2010, Coupling active and passive techniques to control the flow past the square back Ahmed body, Computers & Fluids 39 (2010) 1875–1892.

Bruneau H. C., Mortazavi I., 2008, Numerical modelling and passive flow control using porous media, Computers & Fluids 37 (2008) 488–498.

Barros D., Borée J., Noack B.R., Spohn A., Ruiz T., 2017, Effects of Unsteady Coanda *Blowing* on the Wake and *Drag* of a Simplified Blunt Vehicle, Springer International Publishing Switzerland 2017.

Beratlis N., Balaras E., Squires K., 2014, Effects of *dimple*s on laminar boundary layers, *Journal of Turbulence*, 2014 Vol. 15, No. 9, 611–627.

Beves C., Barber C, leonardi T. J. E., 2011, Aerofoil flow separation suppression using *dimple*s, Aeronautical Journal 2011, vol. 115, n^{o}1168, pp. 335-344.

Chear C. K., S. S. Dol, 2015, Vehicle Aerodynamics: *Drag* Reduction by Surface *Dimple*s, International Journal of Mechanical, Aerospace, Industrial, Mechatronic and Manufacturing Engineering Vol:9, No:1, 2015

Gilleron P., Chometon F., 1999, Modelling of stationary three-dimensional separated air flows around an Ahmed reference model, ESAIM Proceedings.

Gillieron P., Kourta A., 2009, Aerodynamic *drag* reduction by vertical splitter plates, Experiments in fluids.

Gillieron P., Leroy A., et al, 2010, Influence of the slant angle of 3 D bluff bodies on longitudinal *vortex* formation, Journal of fluids Engineering.

Gillieron P., Kourta A., 2013, Aerodynamic *drag* control by pulsed jet on simplified car geometry, Experiments in fluids.

Harinaldi, Budiarso, Tarakka R., Simanungkalit SP, 2011, Computational analysis of active flow control to reduce aerodynamics *drag* on a van model, International Journal of Mechatronics Engineering IJMME-IJENS Vol: 11 No : 03

Harinaldi, Budiarso, Warjito, Kosasih E. A., Tarakka R., 2013, Active technique by suction to control the flow structure over a van model, American Institute of Physics.

Harinaldi, Budiarso, Tarakka R., Simanungkalit S. P., 2013, Effect of Active Control by *Blowing* to Aerodynamic *Drag* of Bluff Body Van Model, International Journal of Fluid Mechanics Research, Vol. 40, No. 4, 2013.

Kim D., Lee H., Yi W., Choi H., 2016, A bio-inspired device for *drag* reduction on a three-dimensional model vehicle, IOP Publishing Bioinspir. Biomim. 11 (2016) 026004.

Kourta A., Gillieron P., 2008, Impact of the automotive aerodynamic control on the economic issues, Journal of applied fluid mechanics, vol. 2. No. 2 pp.69-75,2009.

Livya E., Anitha G., Valli P., 2015, Aerodynamic Analysis of *Dimple* Effect on Aircraft Wing, International Journal of Mechanical, Aerospace, Industrial, Mechatronic and Manufacturing Engineering Vol:9, No:2, 2015.

Leclerc C., Levallois E., et al, 2006, Aerodynamic *drag* reduction by syntetic jet : A 2D Numerical study around a siplified car, 3rd AIAA Flow control Conference.

Lehugeur B., Gillieron P., Kourta A., 2010, Experimental investigation on longitudinal vortes control over a dihedral bluff body, Experiments in Fluid.

Moussa A. A., Fischer J., Yadav R., 2015, Aerodynamic *Drag* Reduction for a Generic Truck Using Geometrically Optimized Rear Cabin Bumps, Hindawi Publishing Corporation Journal of Engineering Volume 2015, Article ID 789475, 14 pages.

Minelli G., Krajnovic S., 2015, Numerical Investigation of the Actuated Flow on a Bluff Body, Springer International Publishing Switzerland 2016 A. Segalini (ed.), *Proceedings of the 5th International Conference on Jets, Wakes and Separated Flows (ICJWSF2015)*.

Minelli G., Noack B. R., Krajnovi S., Basara B., 2016, Numerical Investigation of Active Flow Control Around a Generic Truck A-Pillar, Flow Turbulence Combust.

Manosalvas D. E., Economon T. D., 2016, Computational Design of *Drag* Diminishing Active Flow Control Systems for Heavy Vehicles, AIAA Aviation 13-17 June 2016, Washington, D.C. 8th AIAA Flow Control Conference.

Munson B, 2002, Mekanika Fluida (Dr.Ir. Harinaldi & Budiarso, M.Eng, Penerjemah), Erlangga, Jakarta

EA Kosasih, H Harinaldi, R Trisno - 2015, Karakteristik pembentukan cincin vorteks pada jet sintetik akibat perubahan frekwensi eksitasi pada aktuator ber-cavity kerucut, Proceeding SNTTM XIV.

Pankajakshan R., Hilbert C. B., Whitfield D. L., 2016, Passive Devices for Reducing Base Pressure *Drag* in Class 8 Trucks, Springer International Publishing Switzerland 2016 A. Dillmann and A. Orellano (eds.), *The Aerodynamics of Heavy Vehicles III*.

Seifert A. , Dayan I. , Horrell C. , Grossmann J., Smith A., 2015, Heavy Trucks Fuel Savings Using the SaOB Actuator, The Aerodynamics of Heavy Vehicles III Volume 79 of the series Lecture Notes in Applied and Computational Mechanics pp 377-390 Universiti Teknikal Malaysia Melaka.

Sarkar S, Thummar K, Shah N, Vagrecha V, 2019 A Review paper on Aerodynamic *Drag* Reduction and CFD Analysis of Vehicles, International Research Journal of Engineering and Technology (IRJET) Volume: 06 Issue: 01 Januari 2019

Tarakka R., Harinaldi, Budiarso, 2012, Pengaruh Ukuran Grid dan Model Turbulensi pada Analisis Komputasi *Drag* Aerodinamika *Bluff Body* Model Kendaraan, Proceeding SNTTM XI) & Thermofluid IV UGM.

SF Wong, SS Dol I, 2016, Simulation study on vihechle *Drag* Reduction by Surface *Dimple*s, International Journal of Mechanical, Aerospace, Industrial, Mechatronic and Manufacturing Engineering Vol:10, No:3, 2016

Tunay T., Yaniktepe B., Sahin B., 2016, Computational and experimental investigations of the vortical flow, structures in the near wake region downstream of the Ahmed vehicle model, J. Wind Eng. Ind. Aerodyn. 159 (2016) 48–64

Voskoboinick V. A., Turick V. N., Voskoboinyk O. A., Voskoboinick A. V. and Tereshchenko I. A. 2019, Influence of the Deep Spherical *Dimple* on the Pressure Field Under the Turbulent Boundary Layer, Springer International Publishing AG, part of Springer Nature 2019

Wang H.F., Mengxia X., 2012, Control of the aerodynamic *drag* of Ahmed model with slot jet, The Seventh International Collquium on Bluff Body Aerodynamics and Applications (BBAA7).

Yingli R, Noack B.R., Cordi er L., Bor.ee J. A., Harambat F., Kakaiser E., Thomasduiez, 2016, *Drag* reduction of a car model by linear genetic programming control, Submitted manuscript physics.flu-dyn.

DAFTAR PUBLIKASI

1. Konferensi nasional KNEP VIII- 2017, Analisa gaya tahanan aliran fluida melintasi pelat berlesung (dimpled) setengah bola konfigurasi sejajar.
2. Jurnal internasional, International Review of mechanicalEngineering (IREME), November 2018 Fluid flow resistance hemispherical dimpled plats in parallael dan zigzag configurations
3. Konferensi internasional ISMEVD, IOP Publishing 2019, computational studies of pressure distribution of flow through inline dimpled plate
4. Jurnal internasional, International Journal of Mechanical Engineering and Robotic Reseach, IJMERR, 2021, computational dan experimental investigations of the efficacy of dimple ratio to characteristics of flow on van vehicle models.

Analisis Gaya Tahanan Aliran Fluida Melintasi Pelat Berlesung (*Dimpled*) Setengah Bola Konfigurasi Sejajar

Nasaruddin Salam[1)], Rustan Tarakka[2)], Jalaluddin[3)], Muh.Setiawan[4)]
[1,2,3,4)]Departemen Teknik Mesin Fakultas Teknik Unhas Makassar

Abstrak

Aliran melintasi susunan permukaan berlesung (*dimpled*) setengah bola konfigurasi sejajar, pada permukaan pelat datar merupakan salah satu bentuk yang masih jarang digunakan pada rekayasa struktur dan transportasi. Berbagai aplikasi dari susunan *dimpled* adalah, pada pemukaan sayap pesawat dan permukaan kendaraan berkecepatan tinggi. Metode penelitian dilaksanakan dalam dua tahapan yaitu, dengan program *computer fluid dynamic* (CFD) menggunakan perangkat FLUENT 6.3.26, dan dengan eksperimental dengan menggunakan *wind tunnel*. Pengukuran gaya tahanan dilakukan dengan alat ukur keseimbangan gaya, sedangkan untuk kecepatan aliran dalam wind tunnel menggunakan tabung pitot yang dihubungkan dengan manometer yang telah dikalibrasi dalam skala satuan kecepatan m/s. Benda uji terbuat dari *acrylic* sebanyak 9 (sembilan) buah dengan ukuran panjang 30 cm, lebar 10 cm dan tebal 0,5 cm, sedangkan *dimpled* berbentuk setengan bola dengan ratio (DR) = 0,5. *Dimpled* disusun dalam konfigurasi sejajar dengan jumlah baris adalah (1, 2, 3, 4, 5, 6, 7 dan 8) baris, kemudian seluruh benda uji diberi perlakuan kecepatan aliran yang sama, yaitu 7 (tujuh) tingkat kecepatan (8; 10; 12; 14; 16; 18 & 20) m/s. Penelitian berlangsung dalam daerah aliran turbulen dengan bilangan Reynolds (Re) dari 129.171 sampai dengan 322.928, menunjukkan bahwa penggunaan *dimpled* setengah bola menurunkan gaya tahanan, sebagai contoh pada kecepatan aliran yang sama 16 m/s, tanpa *dimpled* diperoleh gaya tahanan (F_D) = 0,22 Newton dan koefisien tahanan (C_D) = 0,05139, sedangkan dengan *dimpled* 2 baris diperoleh F_D = 0,200 Newton dan C_D = 0,04672, dengan demikian penggunaan *dimpled* 2 baris menurunkan gaya tahanan sebesar 9,087 % pada Re = 258.342.

Kata kunci: *gaya tahanan, pemisahan aliran, pelat berlesung (dimpled).*

Abstract

The flow across the dimpled surface of half-spherical parallel configurations, on the flat plate surface is one of the rarer forms used in structural engineering and transport. Various applications of the dimpled array are, on the wing surface of the aircraft and the surface of high-speed vehicles. The research method is carried out in two stages namely, with computer fluid dynamic (CFD) program using FLUENT 6.3.26 device, and experimentally using wind tunnel. The measurement of the drag force is carried out by means of a force balance gauge, while for flow velocity in a wind tunnel using a pitot tube connected to a calibrated manometer in the unit scale of m/s velocity. The test specimens are made of acrylic as many as 9 (nine) pieces with length of 30 cm, width 10 cm and 0.5 cm thick, while dimpled in the form of ball with the ratio (DR) = 0.5. The dimpled is arranged in parallel configurations by the number of rows (1, 2, 3, 4, 5, 6, 7 and 8) rows, then the entire specimen is treated with the same flow velocity, ie 7 (seven) velocity levels (8, 10, 12, 14, 16, 18 & 20) m/s. The study took place in a turbulent flow region with Reynolds number (Re) from 129,171 to 322,928, indicating that the use of dimpled half-spheres lowered the drag style, For example at the same flow velocity 16 m / s, without dimpled obtained drag force (F_D) = 0.22 Newton and drag coefficient (C_D) = 0.05139, Whereas with dimpled 2 rows obtained F_D = 0.200 Newton and C_D = 0.04672, thus the use of dimpled 2 rows decreases the drag force by 9.087% at Re = 258.342.

Keywords: *drag force, flow separation, dimpled plates.*

1. Pendahuluan

Aliran melintasi susunan permukaan berlesung (*dimpled*) pada permukaan pelat datar merupakan salah satu bentuk yang masih jarang digunakan pada rekayasa struktur dan transportasi. Berbagai aplikasi dari susunan *dimpled* pelat datar adalah, pada pemukaan sayap pesawat dan permukaan kendaraan berkecepatan tinggi. Ketika suatu fluida mengalir melalui suatu pelat datar, maka akan terjadi kehilangan energi akibat adanya gaya tahanan yang ditimbulkan oleh pengaruh lapisan batas dan oleh adanya pemisahan aliran (*separasi*). Dalam kategori pertama, tahanan disebabkan secara langsung oleh efek-efek viskos sehingga tegangan tangensial disebut tahanan viskos atau tahanan gesek. Kategori ke dua, walaupun secara tak langsung disebabkan oleh viskositas, namun disebabkan karena pengaruh tekanan, jadi karena gaya-gaya normal dan disebut tahanan bentuk atau tahanan tekanan. Hal ini merupakan salah satu permasalahan yang dihadapi industri transportasi dalam meningkatkan efisiensi dan stabilitas sistem.

Aliran turbulen melintasi barisan *dimpled* pada sebuah saluran dengan bilangan Reynolds rendah, pada empat kedalaman (h) yaitu (0,05; 0,10; 0,15 dan 0,2) mm, menunjukkan fluktuasi *near wall turbulent* dapat efektif secara signifikan oleh cosinus bentuk *dimpled*. Pada *dimpled* yang lebih dalam, lebih besar separasi aliran yang terjadi pada rongga dan tegangan Reynolds yang dihasilkan pada *near wall turbulent* diikuti oleh tekanan *drag* dan total *drag* yang lebih besar [1].

*Korespondensi: Tel./Fax.: 082347781915
E-mail: nassalam.unhas@yahoo.co.id

Penggunaan *dimpled* seperti tonjolan atau cekungan pada sayap pesawat, telah terbukti bermanfaat sebagai penyebab penurunan *drag* tekanan dan menunda pemisahan aliran. Mengoptimalkan penempatan beberapa *dimpled* di *trailing edge* sayap, untuk menjaga lapisan batas melekat. Optimasi dalam hal ukuran, bentuk dan desain *dimpled* telah dilakukan untuk meningkatkan efisiensi sayap. Untuk *semi-spherical* cekung, dan semi-spherical cembung dan konfigurasi komposit cekung telah dilakukan untuk menentukan efektivitas maksimum yang dapat dicapai dalam menunda batas pemisahan lapisan di *trailing edge*. Model uji menggunakan Boeing 737 *mid-wing* bagian *airfoil*, untuk mengoptimalkan desain *dimpled* dalam penggunaan praktis desain sayap komersial, dan untuk mencapai efisiensi yang lebih aerodinamis serta pengurangan *stall* [2].

Pada *dimpled* berukuran mikro yang diukir ke permukaan logam menggunakan metode modifikasi *ultrasonic nano-crystal surface*, lapisan batas turbulen melewati permukaan *dimpled* dan berkembang di belakang *trailing edge* pelat datar diukur dengan teknik pengukuran aliran dan mengungkapkan penambahan momentum aksial dalam lapisan batas. Permukaan *dimpled* dengan kekasaran skala *submicron* mengalami *hydrophobicity* permukaan. Formasi *dimpled* dapat mengurangi *skin friction* dengan mereduksi tegangan geser pada dinding serta mereduksi profil *drag* sekitar 3-5% secara konsisten, dan ditemukan bahwa *dimpled manufacturing* memberikan permukaan akhir yang lebih baik karena mengurangi gaya *drag* [3].

Koefisien gesekan-dinding aliran lapisan batas turbulen melewati dinding licin dengan alur persegi melintang pada empat konfigurasi dinding-beralur. Empat konfigurasi dinding-beralur tersebut, seperti dinding yang kasar, yang ditandai dengan spasi rongga persegi dua dimensi (alur) ditempatkan normal terhadap aliran. Integrasi koefisien gesekan-dinding dalam arah aliran menunjukkan bahwa ada peningkatan *drag* total hinggai 3,54 % pada alur tunggal [4].

Pendekatan simulasi numerik lapisan batas turbulen melewati tonjolan (*bump*) dilakukan untuk mendapatkan efek dari permukaan kelengkungan *longitudinal* dari fluktuasi tekanan dinding. Fluktuasi dinding tekanan secara signifikan meningkat di dekat *trailing edge* pada *bump*, di mana lapisan batas memperoleh gradien tekanan yang sangat merugikan. Struktur skala besar pada distribusi fluktuasi tekanan dinding, diamati berkembang pesat dekat *trailing edge* pada *bump* dan *convect downstream*. Jarak antara vortisitas *streamwise* dan dinding sedikit meningkat pada *trailing edge* pada *bump*. Hal ini disebabkan besarnya vortisitas *streamwise*, untuk meningkatkan secara signifikan berkurangnya interaksi dengan dinding, yang mengarah kepeningkatan fluktuasi tekanan dinding [5].

Konfigurasi *dimpled* dengan diameter 1.0 mm dan rasio kedalaman-diameter 0,2, yang terletak di 30% - 60%; dan 75% - 95% panjang *chord* aksial masing-masing sisi hisap, efektif mengurangi kehilangan tekanan total. Pada sudut datang -5,3°, 0°, 5.3°, 7,5°, 10° dan Bilangan Mach 0,4. Peningkatan gaya beban *blade* yang memiliki *dimpled*. Hasil perbandingan juga menunjukkan bahwa *dimpled* pada 30% - 60% dari sisi hisap lebih efektif dalam mereduksi kerugian tahanan dibanding 75% - 95%, pada semua sudut datang [6].

Karakteristik lapisan batas turbulen melewati permukaan pelat datar yang memiliki *dimpled* dibandingkan dengan tanpa *dimpled*, ditemukan bahwa faktor gesekan pelat memiliki *dimpled* sekitar 30% - 80% lebih tinggi dibandingkan dengan pelat datar, dan tergantung pula pada Bilangan Reynolds. Hal ini menunjukkan fenomena karakteristik aliran melewati permukaan pelat yang memiliki *dimpled* menjadi menarik untuk dikaji [7]. Karakteristik aliran di sekitar bola, maka aliran akan melewati pertumbuhan lapisan batas pelat datar, fenomena ini ditunjukkan secara eksperimental PIV. Bila bola tertanam dalam lapisan batas turbulen, dengan ketebalan 63 mm yang lebih besar dari diameter bola 42,5 mm maka distribusi fluktuasi kecepatan aliran, pola garis arus seksional, kontur vortisitas, medan kecepatan aliran, energi kinetik turbulen dan korelasi tegangan Reynolds dapat diperoleh dengan menggunakan data PIV. Kajiannya menjelaskan bahwa, jet seperti aliran yang memicu aliran *entrainment* antara inti dan interaksi lapisan batas yang berkembang sebagai fungsi lokasi bola. Kesenjangan rasio yang besar mempengaruhi struktur aliran dari batas-berkembangnya interaksi lapisan batas yang berkembang dan variasi lokasi terjadinya separasi aliran permukaan pelat. Pola aliran waktu rata-rata menghasilkan struktur asimetris hilir bola, karena pengaruh distribusi lapisan batas aliran pada bola [8].

Kontrol *passif Dimpled*, memicu ketidakstabilan yang menyebabkan tranport momentum yang signifikan. Lapisan geser terbentuk sebagai separasi aliran melewati dua baris pertama *dimpled* menjadi tidak stabil dan kumpulan *vortex* yang koheren. Ketika *vortex* berkembang melewati pelat atau rangkaian *dimpled* maka dinamika aliran menjadi sangat berbeda akibat perubahan tranport momentum melintasi lapisan batas. Penerapan *dimpled* type *semi spherical inward* pada benda uji pelat, dengan rasio *dimple* (RD) 0,1 dan kedalaman *dimpled* setara dengan dua kali tebal lapisan batas. Formasi *dimpled* 2 dan 8 baris bersilangan (*staggered arrangement*). Hal ini memberikan gambaran fenomena pola aliran yang terjadi pada aliran jika pelat datar mendapatkan penambahan *dimpled* dipermukaannya [9]

2. Metode Penelitian

2.1. Rumus Koefisien Tahanan Aliran

Untuk menentukan nilai koefisien tahanan dan menggambarkan karakteristik aliran fluida melintasi plat berlesung setengan bola, maka digunakan rumus: Bilangan Reynolds (Re) [10]:

$$Re = \frac{U.L}{\upsilon} \qquad (1)$$

Re: bilangan Reynolds pada pelat
U : kecepatan aliran udara (m/s)
L : panjang pelat (m)
υ : viskositas udara (m^2/s)

Untuk menentukan Koefisien tahanan (C_D), rumus [10]:

$$C_D = \frac{2 \cdot F_D}{\rho_{ud} \cdot U^2 \cdot A} \qquad (2)$$

C_D : koefisien tahanan
F_D : gaya tahanan (Newton)
w : lebar pelat (m)
A : luas permukaan pelat (m^2) = w.L
ρ_{ud} : massa jenis udara (kg/m^3)

2.2. Model Benda Uji Dan Peralatan Penelitian

Benda uji berbentuk pelat datar dan pelat datar yang ditambahkan formasi *dimpled* dipermukaan atasnya. Permukaan atas pelat datar ditambahkan berbagai variasi konfigurasi formasi *dimpled*. Perlakuan yang diberikan adalah dengan merubah jumlah baris *dimpled* terhadap sumbu x (L_x/D) sebanyak 8 (delapan) tingkat variasi yaitu (1, 2, 3, 4, 5, 6, 7 dan 8) baris dan tanpa *dimpled*, dengan jarak antar *dimpled* terhadap sumbu z (L_z/D) konstan, rasio *dimpled* (DR = 0,5) dengan bentuk *dimpled* setengah bola. Setiap konfigurasi barisan *dimpled* dipasang sejajar, kemudian dialiri fluida yaitu udara dalam 7 (tujuh) tingkat kecepatan aliran (Uo) yang sama. Perlakuan tingkat kecepatan aliran (Uo) yang dimaksud adalah, 8 m/s, 10 m/s,12 m/s, 14 m/s, 16 m/s, 18 m/s, dan 20 m/s.

Material benda uji pelat datar yang digunakan adalah *acrylic* dengan ketebalan 5 mm. Pembentukan kompigurasi *dimpled* menggunakan mesin CNC. Adapun ukuran benda uji pelat datar adalah, masing-masing panjang (L) = 300 mm), lebar (w) = 100 mm, dan tebal (h) = 5 mm.

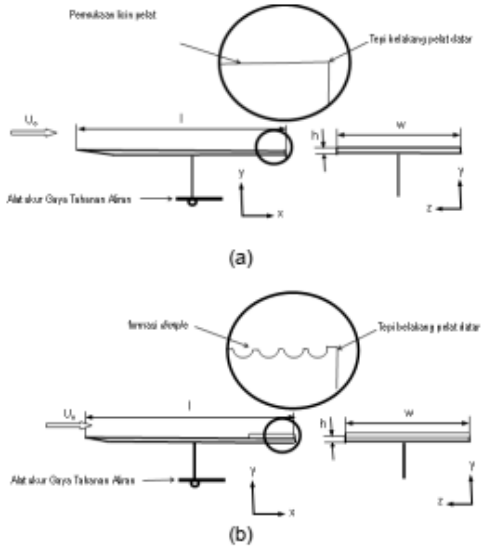

Gambar 1 Benda uji (a) permukaan licin pelat datar (tanpa *dimpled*), (b) permukaan pelat datar dengan penambahan formasi *dimpled*.

Dari gambar 1 terlihat bahwa pemasangan dimpled pada pelat adalah pada ujung bagian belakang pelat datar.

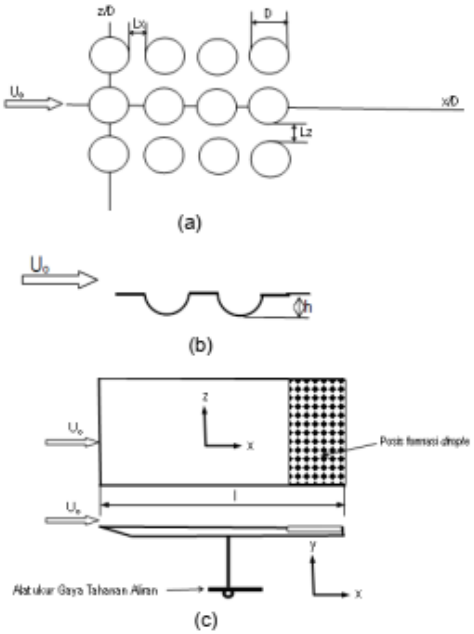

Gambar 2 Tampakan *Dimpled* konfigurasi sejajar (a) tampak atas, (b) tampak samping, dan (c) posisi peralatan penelitian dan alat ukur gaya tahanan aliran.

Dari gambar 2 memperlihatkan konfigurasi baris *dimpled* yaitu, pada gambar 2(a) sumbu z horizontal yang tegak lurus terhadap arah aliran, dan sumbu x searah sumbu aliran. Jarak antara *dimpeld* pada sumbu x (L_x) dan jarak antar *dimpled* pada sumbu z (L_z). Kedalaman setengah bola *dimpled* (H) sebagaimana diperlihatkan dalam gambar 2(b), sedangkan gambar 2(c) memperlihatkan posisi alat ukur gaya tahanan. Untuk pengukuran kecepatan aliran, digunakan manometer yang merupakan paket peralatan *wind tunnel* yang telah dikalibrasi, sehingga skala yang terbaca langsung dalam satuan m/s [11].

2.3. Tahapan Analisis

Tahap awal analisis adalah dengan pendekatan komputasi dengan *software CFD Fluent 6.3*, dengan tujuan untuk mengetahui pengaruh gaya tahanan (*drag*) aerodinamika aliran melintasi benda yang diberi perlukuan bentuk, berupa variasi konfigurasi baris *dimpled* yang sejajar. Model turbulensi *k-epsilon standard* yang digunakan pada simulasi komputasi.

Tahapan analisis selanjutnya adalah, dengan melakukan eksperimental yaitu, dengan menggunakan peralatan pengujian standar internasional berupa terowongan angin (*wind tunnel*) yang ada di Laboratorium Mekanika Fluida Departemen Teknik Mesin Fakultas Teknik Universitas Hasanuddin. Terowongan angin (*wind tunnel*) yang digunakan dalam eksperimen ini adalah buatan Plint & Partners LTD Engineers, dimana kecepatan aliran udara melalui seksi uji dengan ukuran (300 mm x 300 mm) maksimum 20 m/s [11].

3. Hasil dan Pembahasan

3.1. Simulasi Komputasi Dengan Program CFD

Gambar 3 berikut ini memperlihatkan *pathline* kecepatan tanpa dimpled pada kecepatan 20 m/s. Dari Gambar 3 tersebut, terlihat bahwa pada bagian belakang model pelat tanpa dimpled terjadi pemisahan aliran pada bagian belakang pelat. Olakan aliran lebih besar dan berlangsung cukup lama. Selanjutnya pada gambar 4 memperlihatkan *pathline* kecepatan dengan dimpled model 2 (dua) baris pada kecepatan yang sama yaitu 20 m/s. Ternya olakan aliran yang terjadi pada model 2 baris lebih kecil dan berlangsung cukup singkat bila dibandingkan tanpa dimpled. Sedangkan, pada gambar 5 memperlihatkan *pathline* kecepatan dengan dimpled model 6 (enam) baris pada kecepatan yang sama yaitu 20 m/s. Ternyata olakan aliran yang terjadi pada model 6 baris lebih besar dan berlangsung cukup lama dibanding dengan model 2 baris dimpled.

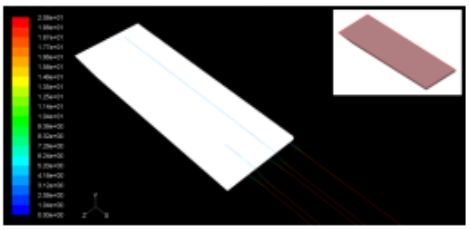

Gambar 3 Pathline kecepatan pada pelat tanpa lesung (*dimple*) dengan kecepatan aliran, U_o = 20 m/s

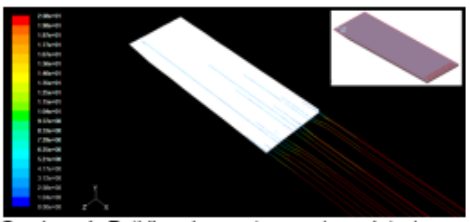

Gambar 4 Pathline kecepatan pada pelat dengan konfigurasi Dimple 2 Baris sejajar, Rasio Dimple, DR=0,5 dengan kecepatan aliran, U = 20 m/s

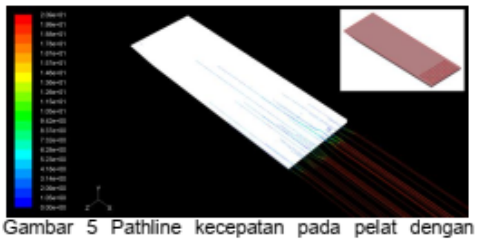

Gambar 5 Pathline kecepatan pada pelat dengan konfigurasi Dimple 6 Baris sejajar, Rasio Dimple, DR=0,5 dengan kecepatan aliran, U = 20 m/s

Berdasarkan ketiga model simulasi CFD tersebut, maka diperoleh model dengan susunan 2 (dua) baris *dimpled* yang terbaik untuk diaplikasikan, atau model ini memiliki gaya tahanan yang paling kecil.

3.2. Pengujian Gaya Tahanan

Hasil eksperimen aliran udara melintasi pelat datar berlesung (*dimpled*) setengah bola konfigurasi sejajar, diperoleh nilai gaya tahanan (F_D) aliran udara pada penggunaan *dimpled* dengan jumlah baris (N), yaitu 1 sampai dengan 8 baris dan tampa *dimpled*, dengan perlakuan 7 (tujuh) tingkat kecepatan aliran udara (Uo) yang sama yaitu 8 m/s sampai dengan 20 m/s atau pada bilangan Re = 129.171 sampai dengan Re = 322.928, sebagaimana ditunjukkan pada table 1 berikut ini:

Tabel 1 Hasil eksperimen gaya tahanan (F_D) pada pelat tanpa *dimpled* dan dengan *dimpled* pada variasi jumlah baris (N) dan kecepatan aliran (Uo)

Uo (m/s)	Gaya Tahanan (F_D)						
	Tanpa Dimpled	Jumlah Baris Dimpled (N)					
		1	2	3	4	6	8
8	0,060	0,050	0,050	0,055	0,060	0,060	0,060
10	0,090	0,080	0,075	0,085	0,090	0,090	0,090
12	0,130	0,120	0,115	0,125	0,130	0,130	0,130
14	0,170	0,160	0,155	0,160	0,170	0,175	0,175
16	0,220	0,205	0,200	0,210	0,220	0,230	0,230
18	0,280	0,275	0,270	0,275	0,280	0,285	0,290
20	0,350	0,335	0,330	0,340	0,345	0,355	0,355

Dari tabel hasil eksperimen tersebut di atas, selanjutnya dibuat gambar grafik hubungan antara F_D dengan N pada Uo yang konstan, sebagaimana dalam gambar 6 berikut ini.

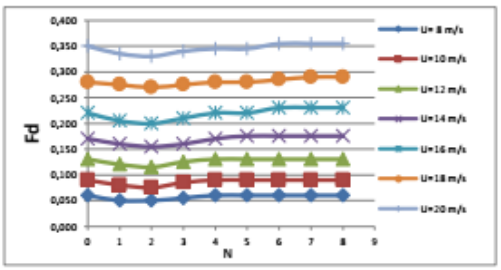

Gambar 6 Hubungan antara Gaya Tahanan (F_D) dengan Jumlah baris dimple (N) pada tujuh tingkat kecepatan aliran (Uo).

Pola karakteristik yang ditunjukkan dalam gambar 6 di atas memperlihatkan bahwa, perubahan kecepatan aliran (Uo) tidak mempengaruhi pola karakteristik F_D terhadap N, yaitu bila N diperbesar, maka nilai F_D semakin kecil, namun demikian pada dimpled dengan 2 baris mengalami titik balik, sehingga untuk semua tingkat Uo diperoleh nilai F_D terkecil pada N = 2 baris. Hal ini menunjukkan bahwa pada N = 2

baris olakan aliran di bagian belakang pelat paling kecil, sehingga pemisahan aliran yang diperoleh terkecil, sebagaimana ditunjukan pada gambar 4 simulasi aliran. Pola karakteristik perubahan gaya tahanan ini, mengikuti pola benda yang diberi gangguan pada silinder persegi tersusun tandem, yaitu bila posisi gangguan tepat maka akan menurunkan gaya tahan aliran benda tandem [12].

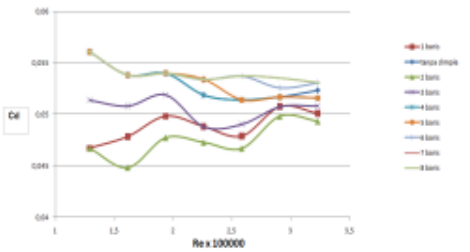

Gambar 7 Hubungan antara Koefisien Tahanan (C_D) dengan Bilangan Reynolds (Re) pada delapan tingkat baris dimpled.

Pola karakteristik yang ditunjukkan pada gambar 7 di atas memperlihatkan bahwa, perubahan jumlah baris (N) secara umum tidak mempengaruhi pola karakteristik F_D terhadap bilangan Reynolds (Re), yaitu bila Re diperbesar, maka nilai C_D semakin kecil, namun demikian pada dimpled dengan 1 dan 2 baris mengalami pola yang berbeda pada bilangan Feynolds yang rendah. Untuk semua variasi bilangan Reynods diperoleh Nilai C_D terkecil pada N = 2 baris. Secara umum semua benda bila dialiri fluida akan mengalami penurunan C_D bila bilangan Reynolds diperbesar [10].

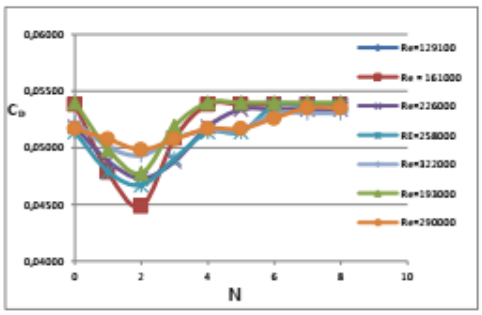

Gambar 8 Hubungan antara Koefisien Tahanan (C_D) dengan Jumlah baris *dimpled* (N) pada tujuh tingkat Bilangan Reynolds (Re).

Pola karakteristik yang ditunjukkan dalam gambar 8 di atas memperlihatkan bahwa, perubahan bilangan Reynokds (Re) tidak mempengaruhi pola karakteristik C_D terhadap N, yaitu bila N diperbesar, maka nilai C_D semakin kecil, namun demikian pada *dimpled* dengan 2 baris mengalami titik balik, sehingga untuk semua tingkat Re diperoleh nilai C_D terkecil pada N = 2 baris. Hal ini menunjukkan bahwa pada N = 2 baris olakan aliran di bagian belakang pelat paling kecil, sehingga pemisahan aliran yang diperoleh terkecil, sebagaimana ditunjukan pada gambar 4 simulasi aliran. Pola karakteristik perubahan koefisien tahanan ini, mengikuti pola karakteristik aliran melintasi benda yang diberi gangguan pada silinder persegi tersusun tandem, yaitu bila posisi gangguan tepat maka akan menurunkan koefisien tahan aliran benda tandem [13].

4. Simpulan

Analisis gaya tahanan aliran fluida melintasi pelat berlesung (*dimpled*) setengah bola konfigurasi sejajar, pada jumlah baris *dimpled* (N) = 1 sampai dengan 8 dan tanpa *dimpled*, dengan kecepatan aliran masuk *wind tunnel* atau aliran luar benda uji Uo = (8 sampai dengan 20) m/s atau aliran turbulen pada bilangan Reynolds Re = 129.171 sampai dengan 322.928, disimpulkan:

a. Semakin besar jumlah baris *dimpled*, maka semakin kecil pula gaya tahanan, namun pada N = 2 mengalami titik balik atau bila N > 2 maka gaya tahanan semakin besar. Nilai gaya tahanan terkecil adalah F_D = 0,200 Newton pada kecepatan aliran Uo = 16 m/s. Fenomena ini, sama dengan yang ditunjukkan pada simulasi komputer dengan program CFD.
b. Semakin besar nilai bilangan Reynolds (Re_D), maka nilai koefisien tahanan (C_D) semakin kecil pada setiap variasi jumlah baris dimlped, namun demikian pada Re yang sama, nilai koefisien tahanan terkecil (C_D = 0,06724) pada N = 2 baris dan Re = 258.342.
c. Pola reduksi gaya tahanan dan koefisien tahanan, mendekati sama untuk setiap perubahan kecepatan aliran atau bilangan Reynolds dan jumlah baris *dimpled*. Fenomena ini menunjukkan bahwa, secara umum penggunaan *dimpled* lebih baik dibanding tanpa *dimpled*.
d. Penambahan jumlah baris dimpled, mereduksi gaya tahanan aliran pada N ≤ 2 namun pada N > 2, maka gaya tahanan semakin besar, hal ini terjadi untuk seluruh tingkat atau perubahan bilangan Reynolds. Fenomena ini menunjukkan bahwa, penggunaan *dimpled* 2 baris menurunkan gaya tahanan sebesar 9,087 % pada Re = 258.342.

Ucapan Terima Kasih

Penelitian ini dibiayai oleh Kementerian Riset, Teknologi dan Pendidikan Tinggi melalui skema Penelitian Unggulan Perguruan Tinggi (PUPT) Tahun Anggaran 2017, dengan Kontrak Penelitian Nomor : 2774/UN4.21/LK23/2017 tanggal 4 Mei 2017.

Daftar Pustaka

[1] Mingwei G.E., *Numerical Investigation of Flow Characteristics Over Dimpled Surface,* Thermal Science Vol: 20, No. 3, pp. 903-906, 2016.

[2] Baweja C., Dhannarapu R., Niroula U., Prakash I., *Analysis and Optimization of Dimpled Surface Modified for Wing Planforms,* 7th International Conference on Mechanical and Aerospace Engineering, 2016.

[3] Paik B.G., Pyun Y.S., Kim K.Y., Jung C. M., Kim C. G., *Study on The Micro-Dimpled Surface in Terms of Drag Performance,* Experimental Thermal and Fluid Science 68, pp. 247–256, 2015.

[4] Ranjan P., Paul A. R., Singh A. P., *Computational Analysis of Frictional Drag Over Transverse Grooved Flat Plates,* International Journal of Engineering, Science and Technology, Vol. 3, No. 2, , pp. 110-116, 2011.

[5] Kim J., Sung H. J., *Wall Pressure Fluctuations in a Turbulent Boundary Layer Over a Bump*, AIAA Journal, Vol. 44, No. 7, 2006.

[6] Zhao Y., Lu H., Sun Y., *Experimental Studies of Dimpled Surface Effect on The Performance of Linear Cascade Under Different Incidence Angles,* 9th International Conference on Digital Enterprise Technology – DET, pp. 137 – 142, 2016.

[7] Zhou W., Rao Y., Hu H., *An Experimental Investigation on the Characteristics of Turbulent Boundary Layer Flows Over a Dimpled Surface,* Journal of Fluids Engineering, Vol. 138, pp. 021204-1 – 13, 2016.

[8] Ozgoren M., Okbaz A., Dogan S., Sahin B., Akilli H., *Investigation of Flow Characteristics Around a Sphere Placed in a Boundary Layer Over a Flat Plate*, Experimental Thermal and Fluid Science 44, 2013 pp. 62–74, 2013.

[9] Beratlis N., Balaras E., Squires K., *Effects of Dimples on Laminar Boundary Layers,* Journal of Turbulence, Vol. 15, No. 9, pp. 611–627, 2014.

[10] Olson M., Reuben, *Dasar-Dasar Mekanika Fluida*, Edisi Kelima, PT. Gramedia Pustaka Utama, Jakarta, 1993.

[11] Plint & Partner LTD Engineer, *Manual Educational Wind Tunnel*, England, 1982.

[12] Salam Nasaruddin, Tarakka Rustan, Jalaluddin, *Reduksi Tahanan Aliran Fluida Melintasi Silinder Persegi Tersusun Tandem Dengan Penambahan Inlet Disturbance Body (IDB),* Prosiding Seminar Nasional ke 3 Rekayasa Material, Sistem Manufaktur dan Konversi Energi, Jurusan Teknik Mesin Fakultas Teknik Unhas Makassar, Halalaman 143-147. ISBN: 978-979-18011-2-6, 2016.

[13] Salam Nasaruddin, Tarakka Rustan, Jalaluddin, Bachmid Reza, *The Effect of the Addition of Inlet Disturbance Body (IDB) to Flow Resistance through the Square Cylinders Arranged in Tandem,* International Review of Mechanical Engineering (I.RE.M.E.), Vol. 11, N. 3, ISSN 1970 – 8734, 2017.

Nasaruddin Salam menyelesaikan pendidikan S1 Teknik Mesin di Universitas Hasanuddin pada tahun 1984, dengan area riset karakteristik aliran fluida dalam pipa, nosel dan fan. Pendidikan S2 Magister Teknik Mesin diselesaikan di Universitas Hasanuddin pada tahun 1999, dengan area riset tentang tebal lapisan batas melintasi benda dan pengaruh perubahan aspek ratio terhadap koefisien tahanan benda.

Pada tahun 2014 menyelesaikan pendidikan S3 Doktoral Teknik Mesin di Universitas Brawijaya Malang. Saat ini ia bekerja sebagai dosen di Departemen Teknik Mesin Universitas Hasanuddin. Bidang penelitian utama yang digeluti adalah aliran fluida melintasi benda tandem, benda yang diberi gangguan dan simulasi aliran dengan program CFD.

Computational studies of pressure distribution of flow through inline dimpled plate

IOP Conf. Series: Materials Science and Engineering **885** (2020) 012022 doi:10.1088/1757-899X/885/1/012022

Computational studies of pressure distribution of flow through inline dimpled plate

M Setiawan Sukardin[1,2], Nasaruddin Salam[2], Rustan Tarakka[2], Jalaluddin Haddade[2], and Muhammad Ihsan[3]

[1]Politeknik ATI Makassar, Indonesia
[2]Department of Mechanical Engineering, Hasanuddin University, Gowa, Indonesia
[3]Sekolah Tinggi Teknik Baramuli, Pinrang, Indonesia

Email: setiawan_mkz@yahoo.co.id

Abstract. Dimple plates are widely used for construction and vehicles, especially in car bodies, trains, and aircraft wings. The dimples surface helps to overcome turbulent airflow around vehicles, thereby delaying the separation point and producing fewer vertices and drag. This study aims to predict the pressure distribution occurring over the plate surface with the formation of inline dimple rows on the upper back end. The test is carried out with Computational Fluid Dynamic (CFD) FLUENT program. The test model has a dimension of 300 mm in length, 100 mm in width, and dimples ratio (DR) of 0.5. Dimples are arranged inline as much as 1 to 6 rows. Upstream velocities through dimple plates range from 10 m/s to 20 m/s. The results of the study show that the minimum pressure coefficient occurs at the top front of the plate due to the flow separation that occurs at the front end of the plate. At x/L=0.25 x/L=0.5 and x/L=0.75 (before the dimples formation), a flow pattern returns to normal, this can be seen from the distribution of the relative pressure coefficient that does not change. At the measurement point x/L=0.95 (after dimples formation), there is a decrease in the pressure coefficient. This decrease occurs due to changes in flow characteristics. The pressure coefficient does not change significantly in dimple variations of 2 to 4 rows. Meanwhile, the pressure coefficient decreases with the variation of the 5 and 6-row dimples.

1. Introduction

Recent developments in the vehicle have heightened the need for aerodynamic drag reduction. There have been studies concerning the development of the method for surface friction drag reduction, and the efforts have progressed widely in two ways: methods for delaying the transition of the laminar-turbulent boundary layer and methods for changing or adjusting the structure of turbulent boundary layer [1]. Passive techniques that have been extensively investigated for turbulent drag reduction include dimples formation on the body surface. The dimpled surface on a golf ball is a well- known application of a non-smooth surface for drag reduction [2]. Several attempts have been made to investigate the reduction in the aerodynamic drag of a vehicle using dimple surface. Wang et al. have conducted numerical studies on generic vehicles to optimize aerodynamic drag using dimple arrays [3]. The dimples surface helps turbulent airflow around the vehicle, thereby delaying the separation point and producing smaller wake and lower form drag. Livya et al. (2015) have evaluated aircraft airfoil drag at 0° - 20° variation angle of attack, which

applies the formation of one dimple [4]. Types of dimples that are applied include square, semi-spherical, compound (a combination of semi-spherical and square) each in the form of concave (inward), and convex (outward). The flow through the dimples forms a small separation bubble. Bubble formation accelerates flow between dimples on the airfoil surface and the boundary layer changes from laminar to turbulent. This transition flow delays the occurrence of flow separation as a cause of decreased drag. Other studies have applied dimple rows on the edge of the back of the Ahmed body with a surface inclination of 25°. The computational approach used is the k-epsilon model on ANSYS Fluent. Dimple ratio variation (DR) were 0.005, 0.2, 0.4 and 0.5 at a speed of 40 m/s where the greatest drag reduction of 1.95% were obtained in the DR 0.4 when compared to the model without dimples [5]. In another study, Zhou et al. (2016) have examined the flow of fluid across the surface of the dimples, with the distribution of surface pressure coefficients measured in a dimple with respective Reynolds numbers; Re=8.2K, Re=36.7K Re=50.5K [6]. Computationally and experimentally, airflow resistance through the dimpled plates has been reviewed in inline and zigzag formations with plates without dimples. The smallest Cd in the inline formation occurs in 2 lines of dimples, while the Cd in the zigzag formation is 1 row of dimples. Decrease in the percentage of the coefficient of resistance between the plates without dimples and the zigzag formation dimpled plates was 5.88%, while the inline formation dimpled plates were 8.65%. [7].

Large-scale asymmetrical vortex structures are formed inside the dimples. The source is located in the front wall of the dimples. Vortex structure tends to intersect the median dimples. In oscillating motion, large-scale asymmetric vortices are periodically released over the back wall at an angle that increases with increasing flow velocity [8]. Dimple, as a passive control, triggers instability that causes significant momentum transport. The shear layer is formed as the flow separation through the first two lines of dimples becomes unstable, and the coherent vortex collection. When vortex develops through plates or dimples, the dynamics of flow become very different due to changes in momentum transport across the boundary layer on staggered arrangement dimples formation 2 and 8 [9].

Fluid flowing on a curved flat plate causes flow separation and boundary layer changes. Separation is caused by the influence of normal force pressure, which is usually called form drag or pressure drag. This study is expected to predict the pressure distribution as a surface drag caused by variations in the number of inline dimple rows on the plate in the quest of an optimal number of dimple rows on objects that have a significant drag form.

2. Method

The test model is in the form of a plate with inline dimple formation. Each model was applied in a variety of dimples rows. Each plate has a dimple row, which is applied to the plate top, with a variation of 1 to 6 rows of dimple arrays. The x-axis is in line with the direction of flow velocity U_0. The distance between the center of the dimples on the x-axis and y-axis is 9 mm, respectively. Dimples ratio R/D=0.5. The dimensions of the plate are 300 mm long, 100 mm wide and 5 mm thick. Airflow velocities U_0 through the surface of the dimpled plate very successively 10 m/s, 12 m/s, 16 m/s, 18 m/s, and 20 m/s. The tapping position of the measurement of the pressure distribution in the workpiece model were at x/L=0.1 x/L=0.25 x/L=0.5 x/L=0.75 (before the dimples) and x/L = 0.95 (after the dimples).

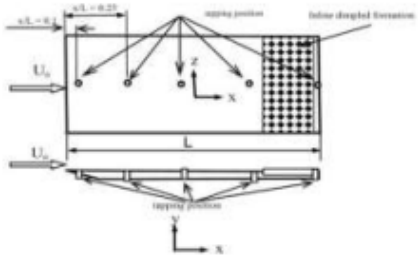

Figure 1. The position of dimples on the plate

Figure 2 illustrates the diameter of the dimples D relative to the distance between the center of the dimple point on the x (Lx) axis and the distance between the center of the dimples on the z-axis (Lz).

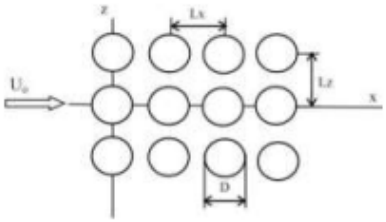

Figure 2. Dimension of inline dimple formation

The computational analysis uses CFD simulation based on ANSYS FLUENT 18.0. The simulation stage starts from drawing the workpiece model using Autodesk Inventor. The meshing process uses ANSYS ICEM CFD 18.0. The assembly of meshing was conducted using tetrahedrons. The number of elements is 1,249,265, and the number of nodes is 227,901. Figure 3 is an example of the result of typical meshing. Figure 4 is a detail of the results of the dimpled plate meshing. The next process is the setup process in ANSYS FLUENT 18.0, simulated in the condition of Re=303K, where air velocity U_0 in a row were 10 m/s, 12 m/s, 14 m/s, 16 m/s, 18 m/s, and 20 m/s on each number of rows dimples. The iteration is attempted to 200 times, followed by the calculation process. Computational results are in the form of pressure distributions at the nodes as measurement points, respectively at x/L=0.1, 0.25, 0.5, 0.75 before the dimples, and 0.95 after the dimples.

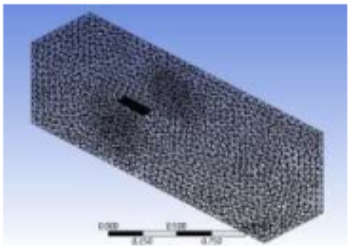

Figure 3. Meshing of test object with 6-row inline dimple formation

Figure 4. Detail of Meshing of the dimpled plate

Pressure drag is the most common form used to define drag on objects. Fluid drag occurs due to the flow, filling the space behind the object, causing a pressure difference between the upstream and downstream flow. Total pressure at the back is lower than that of the front of the object, causing backward suction. The pressure force on flat areas of the plate, which is perpendicular to the flow, causes an enormous drag effect compared to the pressure force on both sides of the flat plate inline to the direction of flow. To acquire the value of this pressure drag force, we need pressure distribution data along the surface of the model. The pressure drag value, a dimensionless parameter, is the coefficient of C_p pressure and commonly expressed as [8].

$$cp = \frac{P-Po}{\frac{1}{2}\rho Uo^2} \qquad (1)$$

p = pressure on the surface of the test model
(Pa) p_o = streamlined pressure or flow line (Pa)
ρ = fluid density
(kg/m^3) U_0 = upstream
speed (m/s)

3. Result and discussion

The present study consists of computational fluid dynamics for variations of the dimple rows on the upper backside of the plate. Upstream velocities range from 10 m/s to 20 m/s. Figures 5 to 9 show that at the measurement point x/L=0.1 (front edge of the plate), there is a decrease in pressure in each test model. It shows that the minimum pressure coefficient occurs on the top side of the front plate due to flow separation that occurs at the front end of the plate. At x/L=0.25, x/L=0.5, and x/L=0.75 (before the dimples formation), the flow pattern returns to normal, which can be seen from the distribution of the relative pressure coefficient unchanged.

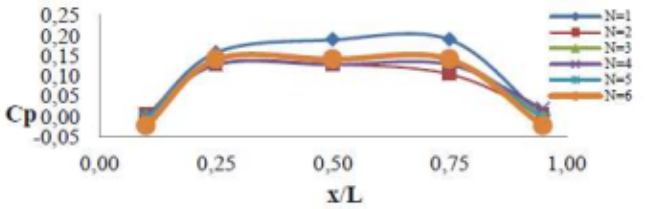

Figure 5. Pressure coefficient for various number of dimple rows of plate with the tapping position, upstream Uo = 10m/s

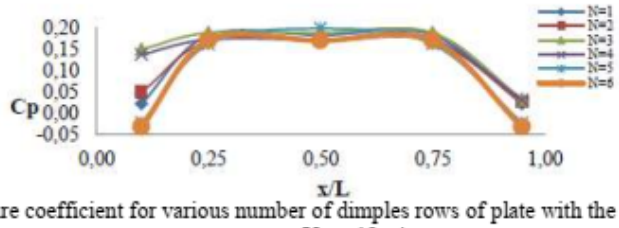

Figure 6. Pressure coefficient for various number of dimples rows of plate with the tapping position, upstream Uo = 12m/s

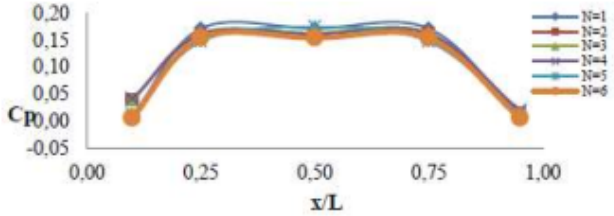

Figure 7. Pressure coefficient for various number of dimples rows of plate with the tapping position, upstream Uo = 14 m/s

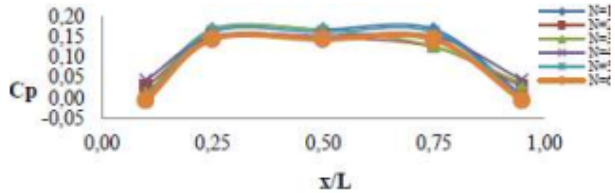

Figure 8. Pressure coefficient for various number of dimples rows of plate with the tapping position, upstream Uo = 16 m/s

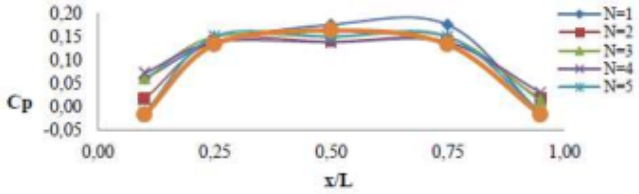

Figure 9. Pressure coefficient for various number of dimples rows of plate with the tapping position, upstream Uo = 18 m/s

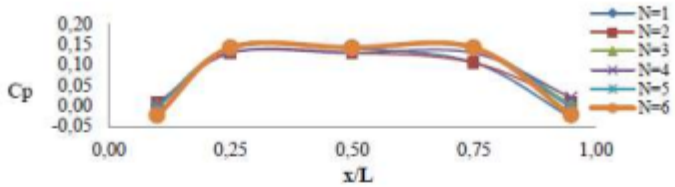

Figure 10. Pressure coefficient for various number of dimples rows of plate with the tapping position, upstream Uo = 20 m/s

Figures 5 to 10 show that at the measurement point x/L=0.1 (front edge of the plate), there is a decrease in pressure in each test model. It shows that the minimum pressure coefficient occurs on the top side of the front side of the plate due to flow separation on the location. At x/L=0.25, x/L=0.5, and x/L=0.75 (before the dimples formation), the flow pattern returns to normal, as indicated by the consistent distribution of the pressure coefficient.

Table 1. Pressure coefficient (C_p) at point after dimple array with x/L=0.95.

Upstream, U_0	Number of dimples rows N					
(m/s)	1	2	3	4	5	6
10	0.001	0.030	0.039	0.032	0.008	0.000
12	0.022	0.025	0.033	0.031	-0.022	-0.032
14	0.009	0.015	0.010	0.020	0.013	0.006
16	0.006	0.027	0.034	0.043	-0.002	-0.007
18	-0.014	0.018	0.013	0.031	-0.012	-0.017
20	-0.029	0.007	0.003	0.020	-0.005	-0.023

From table 1 above, a graph is made of the relationship between the pressure coefficient C_p and the number of dimples N lines in the upstream constant U_0, as in the following figure.

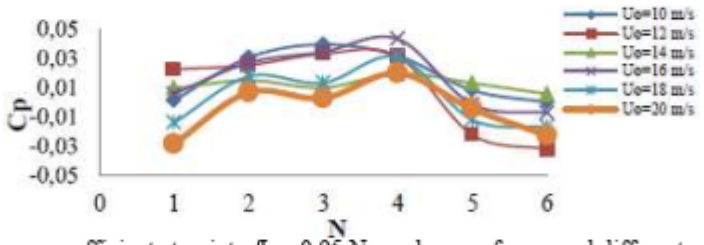

Figure 11. Pressure coefficient at point x/L = 0.95 N number or of rows and different upstream velocity Uo

Figure 11 shows the pressure coefficient at point x/L=0.95 of dimple rows variation at different upstream velocity. The figure also shows that regardless of the variations of the number of rows, no significant change in the pressure coefficient is generated for all upstream speeds. High coefficient of pressure C_p tends to occur in variations of 2 and 4 rows. This shows that the addition of dimple rows up to 4 rows does not contribute to significant friction at the plates. This phenomenon is in line with the smallest coefficient of resistance obtained in 2 rows of dimples [7]. Numbers of rows of 2 to 4 rows can be an alternative to passive flow control, which serves to delay the separation of the surface shape of the objects that change shape drastically, including the shape of the bluff body. Another finding of the research is the development of micro-sized Kelvin-Helmholtz vortex structures over the dimple indentation which confirms the results of Zhou et al. [6]

4. Conclusion

This study concerns to examine numerically the effect of dimple rows in a range of upstream velocity from 10 m/s to 20 m/s on the pressure distribution over a flat plate. From the simulation results, the following conclusions can be drawn. The minimum pressure coefficient occurs at the top front of the plate due to the flow separation that occurs at the front end of the plate. At x/L=0.25, x/L=0.5, and x/L=0.75 (before the dimples formation) a flow pattern returns to normal as indicated by the relatively unchanged distribution of the pressure coefficient. At the measurement point x/L=0.95 (after dimples formation), there is a decrease in the pressure coefficient. This decrease occurs due to changes in flow characteristics. Fluid flow through the surface of the dimple causes low-speed recirculating flow, which produces Kelvin-Helmholtz vortex structures. The pressure coefficient does not change significantly in dimple variations of 2 to 4 rows, whereas in dimple variation of 5 and 6 rows, the pressure coefficient decreases.

Acknowledgments

The authors gratefully acknowledge financial support from the Ministry of the Industry Republic of Indonesia under the 2019 F.Y. Grant.

References

[1] Viswanath P R 2002 Aircraft viscous drag reduction using riblets *Prog. Aerosp. Sci.* **38** 571–600
[2] Alam F, Steiner T, Chowdhury H, Moria H, Khan I, Aldawi F and Subic A 2011 A study of golf ball aerodynamic drag *Procedia Eng.* **13** 226–31
[3] Wang Y, Wu C, Tan G and Deng Y 2017 Reduction in the aerodynamic drag around a generic vehicle by using a non-smooth surface *Proc. Inst. Mech. Eng. Part D J. Automob. Eng.* **231** 130–44
[4] Livya E, Anitha G and Valli P 2015 Aerodynamic analysis of dimple effect on aircraft wing *Int. J. Mech. Aerospace, Ind. Mechatron. Manuf. Eng.* **9**
[5] Wong S F and Dol S S 2016 Simulation Study on Vehicle Drag Reduction by Surface Dimples *Int. J. Mech. Mechatronics Eng.* **10** 560–5
[6] Zhou W, Rao Y and Hu H 2016 An experimental investigation on the characteristics of turbulent boundary layer flows over a dimpled surface *J. Fluids Eng.* **138**
[7] Salam N, Tarakka R, Jalaluddin J and Muh S 2018 Fluid Flow Resistance Through Hemispherical Dimpled Plates in Parallel and Zigzag Configurations *Int Rev Mech Eng IREME* **12**
[8] Voskoboinick V A, Turick V N, Voskoboinyk O A, Voskoboinick A V and Tereshchenko I A 2018 Influence of the deep spherical dimple on the pressure field under the turbulent boundary layer *International Conference on Computer Science, Engineering and Education Applications* (Springer) pp 23–32
[9] Beratlis N, Balaras E and Squires K 2014 Effects of dimples on laminar boundary layers *J. Turbul.* **15** 611–27

Praise Worthy Prize

International Review of Mechanical Engineering (I.RE.M.E.), Vol. 12, N. 11
ISSN 1970 - 8734 *November 2018*

Fluid Flow Resistance Through Hemispherical Dimpled Plates in Parallel and Zigzag Configurations

Nasaruddin Salam, Rustan Tarakka, Jalaluddin, M. Setiawan Sukardin

Abstract – *The application of hemispherical dimples in parallel and zigzag configurations on flat plates flowed with fluids is one of the rarest forms used in structural and transport engineering. It has been particularly studied on aircraft wing, turbine blade, golf balls and vehicle bodies with dents. For this reason, a study on resistance force on hemispheric dimpled in parallel and zigzag configuration on flat plates has been performed. The test piece has been made of acrylic in a total of 9 pieces with length of 30 cm, width 10 cm and thickness of 0.5 cm and dimpled ratio DR = 0.5. Dimples are arranged in rows numbered from 1 to 8. All the specimens are treated in 7 equal flow velocity rates from 8 m/s to 20 m/s. The study, which has taken place in laminar flow region with Reynolds number (Re) of 1.29×10^5 to 3.23×10^5, indicates that the use of hemispherical dimples in parallel and zigzag configuration reduces the resistance coefficient (C_d). For example, in the same $Re=2.26\times10^5$ without dimples obtained C_d has been 0.0517 whereas on plates with dimples in parallel configuration, the smallest resistance coefficient obtained on 2 rows dimples has been of 0.0472. Dimpled plates in zigzag configuration have obtained C_d=0.0487 for single line dimple configuration. When compared with the plates without dimples, the percentage of resistance reduction coefficient for dimpled plates in zigzag configuration is 5.88%, while for dimpled plate in parallel configuration is 8.65%. This result shows that the use of parallel configuration is better than zigzag configuration.*

Keywords: *Resistance Coefficient (C_d), Reynolds Number (Re), Dimpled Plates, Parallel and Zigzag Configuration*

Nomenclature

A	Sectional area of plates
C_d	Drag coefficient
$F_{d_{th}}$	Theoretical drag force
$F_{d_{act}}$	Actual drag force
l	Length of plate
w	Width of plate
h	Length of plate
H	Depth of dimple
Re_L	Reynolds number
U_0	Incoming air flow velocity to wind tunnel
ρ	Air density
υ	Kinematic air viscosity
L_x	Distances between dimples on the x-axis
L_z	Distances between dimples on the z-axis
N	Number of dimple rows
x/D	Ratio of distance in x-axis to diameter of dimple
z/D	Ratio of distance in z-axis to diameter of dimple

I. Introduction

Various applications of dimpled plate arrangement can be found on the surface of aircraft wing and on the surface of high-speed vehicles. When fluid flows through a flat plate, energy losses due to the resistance force generated by the influence of the boundary layer and by the separation of streams will occur. In the first category, the resistance is caused directly by viscous effects. Therefore, the tangential stress is called viscous resistance or friction resistance. In the second category, although indirectly caused by viscosity, resistance is caused by the influence of pressure, i.e. normal forces, and it is called shape resistance or pressure resistance. This is one of the problems on the transportation industry in improving system efficiency and stability. Turbulent flow through arrays of dimples on a channel with a low Reynolds number at four depths (h) i.e. 0.05 mm, 0.10 mm, 0.15 mm and 0.2 mm indicates that near wall turbulent fluctuations can be significantly effective by the shape and the depth of dimples [1]. The use of bump or concave dimples on the wing of the aircraft has been proven to be useful as a factor in decreasing drag pressure and delaying flow separation. Optimizing placements of multiple dimples on the wing trailing edge is useful to keep the boundary layer attached. Optimizations in terms of size, shape and design of dimples have been conducted in order to improve wing efficiency. Research on utilizing concave, convex and composite concave and convex semi-spherical configurations have been performed in order to determine the maximum effectiveness that can be achieved in delaying the layer separation boundary on the trailing edge [2]. Dimples surface with a submicron-scale

 https://doi.org/10.15866/ireme.v12i11.14005

roughness has undergone surface hydrophobicity.

Dimpled formations can reduce skin friction by reducing shear stress on walls and reducing drag profiles by about 3-5% consistently [3]. The integration of the wall-friction coefficient in the flow direction indicates a total drag increment of 3.54% in a single groove [4]. A numerical simulation approach of the turbulent boundary layer passes through the bump has been performed in order to obtain the effect of the longitudinal curve surface to the wall pressure fluctuations. The fluctuation of the pressure wall significantly increases near the trailing edge on the bump where the boundary layer obtains a very adverse pressure gradient [5]. Dimpled configuration of 1.0 mm in diameter with dimpled ratio of 0.2, located on 30% - 60% and 75% - 95% of axial chord lengths on each side of suction has effectively reduced total pressure loss [6]. On characterization of the turbulent boundary layer passes through the surface of the flat plate having dimpled compared with no dimpled, it has been found out that the friction factor of plate with dimples has been higher on about 30% - 80% compared to the one of the flat plate.

The friction factor of the plate also depends on Reynolds number value [7]. When a sphere is embedded in a turbulent boundary layer, the distribution of flow velocity fluctuation, the sectional streamline pattern, the vorticity contour, the flow velocity field, the turbulent kinetic energy and the correlation of the Reynolds pressure can be obtained using PIV data. The large gap of the ratio affects the flow structure of the wake-boundary layer interaction and reattachment location variation of the flow separation[8]. Dimpled passive control can trigger instability that causes significant momentum transport on the application of semi-spherical concave dimples with dimpled ratio (RD) 0.1 and dimpled depth equivalent to twice the thickness of the boundary layer.

The shear layer developing as the flow separation through the first two dimple lines gets unstable and it forms coherent vortex layers. As the vortex evolves through the plates or dimpled series, the flow dynamics become different significantly with remarkable change of momentum transport across the boundary layer [9]. From the analysis on the use of vortex generators in order to improve and control flow characteristics, dimples application have been found out to be useful [10]-[11]. A further improvement has been proposed by incorporating the use of a novel surface modification in the form of dimples inspired by golf ball designs which help to reduce the wake region induced by boundary layer separation [12]. The surface modifications by considering different types and shapes of dimples could help to reduce pressure drag when airfoil reaches a variety of angle. This happens because wake formation initializes due to boundary layer separation. Application of dimples on aircraft wing works in the same way as vortex generators could help to increase the overall aerodynamic characteristics which in turn could enhance the aerodynamic characteristics and maneuverability. The enhancement includes the reduction in drag and stall phenomenon where the airfoil containing dimples will have relatively less drag than the airfoil without dimples. Dimples application on the aircraft wing could create vortices which could delay the boundary layer separation resulting in decreasing of pressure drag and the increasing in the stall angle. Additionally, wake reduction can lead to acoustic emission reduction [13].

Dimples could behave as protrusions on the surface of the wing which could generate vortices resulting in a reduction of flow separation on the suction side of the wing. This can delay and reduce the chord-wise boundary layer growth rate. An experimental analysis on dimple effect carried out on a symmetrical wing has proved the reduction of drag and delaying the flow separation on the upper surface of aircraft wing [14]. Computational and experimental analyses of dimple effect have been studied on aircraft wing using NACA 6321 airfoil. Analyses have been conducted on aerofoil with circle, heart, elliptical type dimples which have been tested under the inlet velocity at different angles of attack. The experiment has showed that the flow separation can be delayed by using dimples on the aerofoil on the aircraft where flow separation in turn reduced the drag. The research which aimed to reduce the take off distance by attaining the high coefficient of the lift at the higher angle of attack has proved that raised pressure drag in wake area at the higher angle of attack has been attained by applying dimples that influence flow separation [15]. Another research has focused on studying the influence of dents on flat plates over the drag coefficient. A total of seven dent configuration, defined by three parameters of dents (depth, main radius, diameter) has been studied for flow conditions of 5 m/s to 40 m/s. The study has been conducted with the help of computational fluid dynamics (CFD) simulations in ANSYS FLUENT where a pre-processing stage such as meshing has been performed in ANSYS Work Bench. Necessary mesh refinement near the plate wall has also been performed to predict the skin friction components. Reynolds Averaged Navier-Stokes (RANS) formulation [21][22] has been used in the simulation with the two-equation SST k-omega turbulence model. The results have showed the drag reduction of nearly 30% by providing dents on the flat plate with flow condition of 10 m/s to 40 m/s [16]. The research on the effect of dimple pattern on the suppression of boundary layer separation on a low-pressure turbine blade has indicated that dimples provide a passive means of controlling boundary layer separation. Determining the optimum and the exact dimple pattern, by advances in the parameterization, in order to totally reduce the boundary layer separation will enormously improve turbine efficiency and it will allow for potentially significant improvements in aircraft mission effectiveness and capabilities [17]. Despite many works have proven that dimple application is useful in reducing energy loss due to fluid flow resistance on bodies such as cars and aircrafts, research works, on determining the formation and number of dimpled lines that could give the optimum reduction of energy loss, have not been available yet. In this regard, hypotheses of the research are parallel dimple configuration is predicted to be more optimum in reducing

the energy loss of fluid flow when compared to zigzag dimple configuration. It is also predicted that there is a particular number of dimple lines which could optimally reduce the energy loss. Following this introduction and subsequent part of methodology, the paper is presenting the results of the research starting with the discussion of parallel dimple configuration, zigzag dimple configuration and followed by the comparison analysis of the two types of configuration. The discussion ends with the verification of the hypotheses which confirms the aforementioned ones.

II. Methodology

The flat plate test piece is added with the dimples in parallel and zigzag configuration on the top surface. The given treatment is to change the number of rows of dimples toward the x axis (L_x/D) by 8 (eight) variation levels (1, 2, 3, 4, 5, 6, 7 and 8) of rows and without dimpled, in order to set distances of dimples to z axis (L_z/D) to be constant, dimpled ratio DR=0.5 with hemi-spherical shape. Each dimple sequence is installed in parallel and zigzag configuration, then flowed in 7 equal flow velocity rates (U_0) which are8 m/s, 10 m/s, 12 m/s, 14 m/s, 16 m/s, 18 m/s and 20 m/s. The flat plate test is manufactured from acrylic material with a thickness of 5 mm while Dimple configuration is formed using a CNC machine with dimensions of 300 mm length (l), 100 mm width (w) and 5 mm thickness (h).

Fig. 1(a) shows the parallel dimple configuration, where the horizontal axis z is designed perpendicular to the flow direction and the x-axis is in the axial flow direction. The distances between dimples on the x axis and z-axis are denoted as L_x and L_z respectively. Fig. 1(b) depicts the zigzag dimple configuration where the hemispheric-dimple depth (H) is shown in Fig. 1(c), while the positioning of the flow resistance force measurement instrument is in Fig. 1(d). For flow velocity measurements, a manometer is used which is a calibrated wind tunnel device package, allowing the scale to be read directly in m/s [18]. The experiment has been carried out using international standard testing equipment in the form of wind tunnel in the Laboratory of Fluid Mechanics, Department of Mechanical Engineering, Faculty of Engineering, Hasanuddin University.

The wind tunnel used in this experiment has been made by Plint & Partners LTD Engineers, where the maximum airflow velocity through the test section with size of 300 mm × 300 mm is 20 m/s [13]. In order to analyze the experimental data from the observation of resistance force as well as to determine the flow characteristics of C_d, $F_{d_{th}}$ and Re due to the addition of the number of lines in each configuration, the following equations are used. Equation (1) is used to determine the coefficient of resistance C_d where the actual or measured resistance force $F_{d_{act}}$ and the theoretical resistance force or air flow $F_{d_{th}}$ have been obtained from Equation (2), whereas ρ and A are the air density and sectional area of plate. Determining the Reynolds number is conducted using Equation (3) where U_0 is the flow velocity across the test specimen, l is the length of the plate and υ is kinematic air viscosity [19]:

$$C_d = \frac{F_{d_{act}}}{F_{d_{th}}} \quad (1)$$

$$F_{d_{th}} = \frac{1}{2}\rho {U_0}^2 A \quad (2)$$

$$Re_L = \frac{U_0 l}{\upsilon} \quad (3)$$

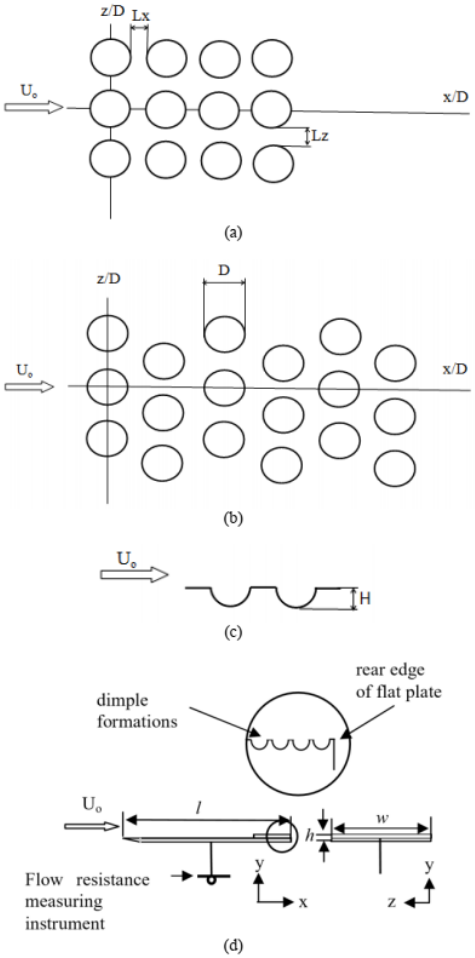

Figs. 1. (a) parallel dimple configuration, (b) zigzag dimple configuration, (c) depth of dimples and (d) positions of equipment and measuring instrument

The study has taken place in the laminar flow region where Reynolds numbers calculated based on the length of the plate are Re_L=1.29×10^5 to 3.23×10^5.

III. Results And Discussion

III.1. Parallel Dimple Configuration

From the experimental results of the airflow across the hemispheric-dimpled plate in parallel configuration, the actual resistance value ($F_{d_{act}}$) of the airflow has been obtained on the use of dimples with the number of rows (N), i.e. 1 to 8 rows and without dimpled, 7 equal airflow velocity levels (U_0) from 8 m/s up to 20 m/s or at the number of Re_L=1.29×10^5 to 3.23×10^5. Furthermore, this value is compared to the one of the theoretical resistance force ($F_{d_{th}}$), then the one of resistance coefficient (C_d) as shown in Table I.

TABLE I
RESISTANCE COEFFICIENT (C_d) FOR PARALLEL CONFIGURATION

Re (10^5)	Resistance Coefficient (C_d)						
	Without Dimpled	Number of Rows (N)					
		1	2	3	5	6	8
1.29	0.0560	0.0467	0.0467	0.0513	0.0560	0.0560	0.0560
1.61	0.0538	0.0478	0.0448	0.0508	0.0538	0.0538	0.0538
1.94	0.0539	0.0498	0.0477	0.0519	0.0539	0.0539	0.0539
2.26	0.0518	0.0488	0.0472	0.0488	0.0533	0.0533	0.0533
2.58	0.0513	0.0478	0.0467	0.0490	0.0513	0.0537	0.0537
2.91	0.0516	0.0507	0.0498	0.0507	0.0516	0.0526	0.0535
3.23	0.0523	0.0500	0.0493	0.0508	0.0515	0.0530	0.0530

Table I indicates that the smallest drag coefficient at all levels of Reynolds number is on the use of 2 dimpled lines. In order to examine the characteristic pattern of each level of Reynolds number, a graph of the relationship between the resistance coefficient (C_d) and the number of rows (N) in the constant Reynolds (Re_L) number is developed, as shown in Fig. 2. The characteristic pattern in Fig. 2 also indicates that the alteration of the Reynolds number has no significant influence to the characteristic pattern of C_d to N, in this condition, when N is enlarged the C_d value shows no increase. However, the dimpled plate with 2 rows has a turning point, where for all the levels of Re, the smallest value of C_d is obtained on N=2 lines.

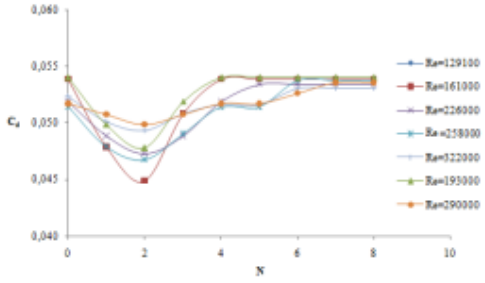

Fig. 2. Relationship between resistance coefficients with the number of lines of parallel dimple configuration for 7 equal levels of Reynolds number

This also indicates that at N=2 lines, the flow wake at the back of the plate is at smallest magnitude, resulting in the smallest flow separation. An interesting fact is that on the number of lines dimple of 4 the C_d, values tend to be constant for each Reynolds number level. This phenomenon shows that a large number of dimple lines is not able to delay the flow separation, so the value of C_d is just slightly larger when compared to the one without dimples.

The characteristic pattern of this alteration of resistance coefficient follows the pattern of objects disturbed in the tandem composed in rectangular cylinders where the exact interference position will decrease the flow resistance coefficient on tandem bodies[20].

III.2. Zigzag Dimple Configuration

Similar treatments are applied on hemispherical dimpled plates in zigzag configuration. The actual drag force ($F_{d_{act}}$) of the airflow is obtained from the application of dimples with the number of rows (N) of 1 to 8 with 7 equal levels of airflow velocity (U_0) varied from 8 m/s up to 20 m/s or on the Reynolds numbers of Re_L = 1.29×10^5 to 3.23×10^5. Similar number of airflow velocity is also applied to plate without dimples. Furthermore, the values are compared to the one of the theoretical resistance force ($F_{d_{th}}$). The value of the resistance coefficient (C_d) is shown in Table II.

TABLE II
RESISTANCE COEFFICIENT (C_d) FOR ZIGZAG CONFIGURATION

Re (10^5)	Resistance coefficient (C_d)						
	Without Dimpled	Number of Rows (N)					
		1	2	3	5	6	8
1.29	0.0560	0.0467	0.0513	0.0560	0.0560	0.0560	0.0560
1.61	0.0538	0.0478	0.0508	0.0508	0.0538	0.0538	0.0538
1.94	0.0538	0.0497	0.0518	0.0518	0.0518	0.0538	0.0538
2.26	0.0517	0.0487	0.0517	0.0502	0.0517	0.0517	0.0532
2.58	0.0512	0.0477	0.0512	0.0501	0.0512	0.0512	0.0524
2.91	0.0515	0.0506	0.0515	0.0515	0.0515	0.0525	0.0534
3.23	0.0522	0.0499	0.0507	0.0507	0.0514	0.0522	0.0529

Table II shows that the smallest drag coefficient of all levels of Reynolds numbers is obtained by the use of 1 dimple line. Based on these results, it is shown that zigzag dimpled configuration does not significantly detract the coefficient of resistance, because on 1 dimple line, the configuration is not really zigzag. In order to examine the characteristic pattern of each level of Reynolds number, a graph of the relationship between the resistance coefficient (C_d) and the number of rows (N) in the constant Reynolds number (Re_L) is developed, as shown in Fig. 3. The characteristic pattern in Fig. 3 shows that Reynolds number change does not affect the characteristic pattern of C_d to N, i.e. when N is enlarged, the C_d value is smaller. However, dimpled plate with 1 row has a turning point, so for all levels of Re, the smallest value of C_d is obtained on N=1 line. This shows that at N=1 line, the flow wake at the back of the plate is smallest, resulting in the smallest flow separation. Another interesting finding is that on the number of lines dimpled by 4, the C_d value tends to be constant for each Reynolds number level.

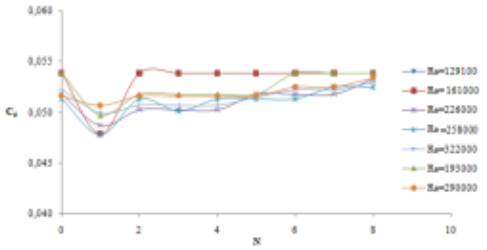

Fig. 3. Relationship between resistance coefficients with number of dimple lines in zigzag configuration for 7 equal levels of Reynolds number

This phenomenon shows that when the number of dimpled lines is added and then a zigzag configuration is formed, the delay the flow separation could not be achieved, so the value of C_d tends to be the same compared to that without dimples. The characteristic pattern of this resistance coefficient change follows the pattern on parallel configuration pattern, but the flow separation has occurred earlier in zigzag configuration.

III.3. Comparison of Parallel and Zigzag Dimple configurations

In order to compare the characteristic pattern of parallel configuration and zigzag configuration, experiments have been conducted at 3 equal levels of Reynolds numbers, as shown in Fig. 4, where the characteristic pattern shown indicates that Reynolds number change does not affect the characteristic pattern of C_d to N, i.e., when the number of N increases, the C_d value is smaller. However,1-row zigzag configuration has a turning point. The parallel dimple configuration with 2 rows also has a turning point. For all Re levels, the smallest C_d value has been obtained on N=1 row on the dimpled plate in zigzag configuration, whereas the smallest C_d value is on N=2 rows on dimpled plate in parallel configuration.

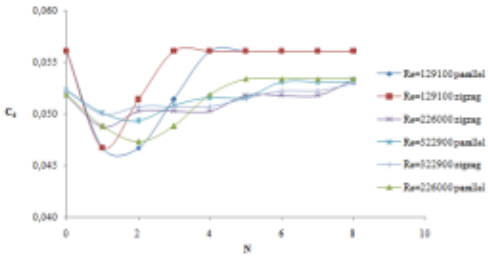

Fig. 4. Relationship between resistance coefficients with the number of lines dimpled parallel configuration and Zigzag at 3 levels of the same Reynolds number

This shows that, the wake of flow in the back of the dimpled plate in parallel configuration is smaller than the one of dimpled plate in zigzag configuration because the flow separation is more delayed. This phenomenon shows that on dimpled plate in 1 line zigzag configuration, resistance coefficient is equal to the one on dimpled plate in 2 lines parallel configuration. At Re_L=2.26×10^5 the smallest C_d value for dimpled plates in 1-row zigzag configuration is 0.048723, while for dimpled plate in 2 rows parallel configuration is 0.047292. For 1-row parallel configuration, C_d is 0.048817. When the result is compared to plates without dimples (C_d=0.051768), the smallest resistance coefficient percentage for dimpled plate in zigzag configuration is 5.88%, while for dimpled plate in parallel configuration, the resistance coefficient is 8.65%.

This result shows that the application of parallel configuration is better than the application of zigzag configuration. This result also shows that it is not necessary to install large numbers of rows of hemispherical dimples on the plate where 1 or 2 rows are sufficient. Because in general the use of flat plates with dimple in zigzag or parallel configurations can be projected on a variety of objects, such as on the aircraft wings, vehicle bodies and blades on fluid machineries, based on the results of the research, the projection will also decrease the drag resistance, which is the main contribution of this research. None of the results of previous research as mentioned in the literature review in the introduction, has applied dimple by giving effect of the number of lines to parallel and zigzag configuration, and none has compared the effect of both configurations which is the novelty of this research. Based on the overall results, the hypotheses that parallel dimple configuration could reduce energy loss on fluid flow more optimally when compared to zigzag configuration is verified. It is also verified that two lines of dimples on plate surface produces the optimum reduction of energy loss.

IV. Conclusion

From the analysis of fluid flow resistance through the hemispherical-dimpled plates in parallel and zigzag configuration, on the number of dimpled rows (N) from 1 to 8 and without dimpled, with the wind tunnel inflows or outer sample flow (U_0) from 8 m/s to with 20 m/s or laminar flow which are on Reynolds number (Re_L) from 1.29×10^5 to 3.23×10^5, it can be concluded:

a. The larger the number of lines dimpled on the parallel configuration is, the smaller the resistance coefficient is, but at N = 2 it has a turning point or when N> 2 the resistance coefficient is larger. The smallest resistance coefficient value is C_d = 0.047292 on the Reynolds number Re_L = 2.26×10^5.
b. The larger the number of dimple lines in the zigzag configuration is, the smaller the resistance coefficient is, but at N = 1 it has a turning point or when N> 1 then the coefficient of resistance is larger. The smallest resistance coefficient value is C_d = 0.048723at Reynolds number Re_L = 2.26×10^5.
c. The resistance coefficient pattern tends to be similar for any alteration in flow velocity or Reynolds number and the number of dimple rows. This phenomenon shows that the use of dimples is better than without

using them.

d. The addition of the number of dimple lines on the plate will reduce the resistance coefficient i.e.5.88%for dimpled plate in zigzag configuration, while for dimpled plate in parallel configuration the reduction is about 8.65%.

Acknowledgements

To the Ministry of Research, Technology and Higher Education, for financing this research through the University Excellence Research Scheme (PUPT) of Fiscal Year 2017, with Research Contract Number: 2774 / UN4.21 / LK23 / 2017 dated May 4, 2017, and to Head of Laboratory of Fluids Mechanics Department of Mechanical Engineering Faculty of Engineering Hasanuddin University, on the permits and facilities provided in the implementation of this research.

References

[1] Mingwei, G. E., 2016. Numerical Investigation of Flow Characteristics Over Dimpled Surface, *Thermal Science*, 20(3). pp. 903-906.

[2] Barveja, C., Dhannarapu, R., Niroula, U., Prakash, I., 2016. Analysis and Optimization of Dimpled Surface Modified for Wing Planforms, *7th International Conference on Mechanical and Aerospace Engineering* 2016.

[3] Paik, B. G., Pyun, Y. S., Kim, K. Y., Jung, C. M., Kim, C. G., 2015. Study on The Micro-Dimpled Surface in Terms of Drag Performance, *Experimental Thermal and Fluid Science*, 68, pp. 247–256.

[4] Ranjan, P., Paul, A. R., Singh, A. P., 2011. Computational Analysis of Frictional Drag Over Transverse Grooved Flat Plates, *International Journal of Engineering, Science and Technology*, 3(2),pp. 110-116.

[5] Kim, J., Sung, H. J., 2006. Wall Pressure Fluctuations in a Turbulent Boundary Layer Over a Bump. *AIAA Journal*, 44(7).

[6] Zhao, Y., Lu, H., Sun, Y., 2016. Experimental Studies of Dimpled Surface Effect on The Performance of Linear Cascade Under Different Incidence Angles, *9th International Conference on Digital Enterprise Technology – DET*, pp. 137 – 142.

[7] Zhou W, Rao Y, Hu H. An Experimental Investigation on the Characteristics of Turbulent Boundary Layer Flows Over a Dimpled Surface. ASME. *J. Fluids Eng.* 2015;138(2). doi:10.1115/1.4031260

[8] Ozgoren, M., Okbaz, A., Dogan, S., Sahin, B., Akilli, H., 2013. Investigation of Flow Characteristics around a Sphere Placed in a Boundary Layer Over a Flat Plate, *Experimental Thermal and Fluid Science* 44, pp. 62–74.

[9] Beratlis, N., Balaras, E., Squires, K., 2014. Effects of Dimples on Laminar Boundary Layers, *Journal of Turbulence*, 15(9), pp. 611–627.

[10] Frank, K. L. and Pierce, A.J., 2011. Review of Micro Vortex Generators in High Speed flow, *49th AIAA AerospaceSciences meeting including the New Horizons forum and Aerospace Exposition*, January 2011.

[11] Storms, B. L., 1994. Lift enhancement of an aerofoil using a gurney flaps and vortex generators, *J. Aircr.*, 31(3), pp 542-547.

[12] Bogdanović-Jovanović, J. B., Stamenković, Ž. M., Kocić, M.M., 2012. Experimental and Numerical Investigation offlow around a sphere with dimples for various flow regimes, *Thermal Science*, 16(4). pp.1013-102.

[13] Mahammi, S.S., 2015. A Review on Study of Aerodynamic Characteristics of Dimple Effect on Wing, *International Journal of Aerospace and Mechanical Engineering*, 2(4), pp.18-21.

[14] Prasath, M. S., Irish A.S. ,2017. Effect of Dimples on Aircraft Wing, *GRD Journals- Global Research and Development Journal for Engineering*, 2(5). pp. 234-241.

[15] Arunkumar, A., Gowthaman, T.S., Muthuraj, R., Vinothkumar, S.,Balaji, K., 2017. Numerical Investigation over Dimpled Wings of anAircraft, *International Journal for Research in Applied Science & EngineeringTechnology (IJRASET)*, 5(4), pp.206-211.

[16] Ahirrao, H., 2016. Numerical Investigation of Drag Reduction on Flat Plates using Dents, *International Journal Of Innovative Research In Technology(IJIRT)*, 3(2), pp.14-19.

[17] Casey, J. P., 2004. *Effect Of Dimple Pattern On The Surpression Of Boundary Layer Separtion On A Low Pressure Turbine Blade*, Thesis, Air Force Institute Of Technology, Wright-Patterson Air Force Base, Ohio.

[18] Plint & Partner LTD Engineer.1982, *Manual Educational Wind Tunnel*, England.

[19] Olson, R. M., S. J. Wright. 1990. *Essentials of Engineering Fluid Mechanics*, 5th Ed., Harper & Row.

[20] Salam, N., Tarakka, R., Jalaluddin, J., Bachmid, R., The Effect of the Addition of Inlet Disturbance Body (IDB) to Flow Resistance Through the Square Cylinders Arranged in Tandem. (2017) *International Review of Mechanical Engineering (IREME)*, 11 (3). pp. 181-190. doi:https://doi.org/10.15866/ireme.v11i3.11338

[21] Kasyanov, P.O., Toscano, L., Zadoianchuk, N.V., A criterion for the existence of strong solutions for the 3D Navier-Stokes equations, (2013) *Applied Mathematics Letters*, 26 (1), pp. 15-17. DOI: 10.1016/j.aml.2012.08.007

[22] Kasyanov, P.O., Toscano, L., Zadoianchuk, N.V., Topological properties of strong solutions for the 3D Navier-Stokes equations, (2014) *Solid Mechanics and its Applications*, 211, pp. 181-187. DOI: 10.1007/978-3-319-03146-0_13

Authors' information

Hasanuddin University.

Nasaruddin Salam–born in Bulukumba on December 20th 1959 is a Professor and the Chairman of Fluid Mechanics Laboratory in Department of Mechanical Engineering, Faculty of Engineering, Hasanuddin University Makassar Indonesia. He holds a doctoral degree from Brawijaya University, Malang Indonesia. His research fields include fluid dynamics particularly on tandem bodies. Prof. Nasaruddin is a member of the Institutions of Engineers Indonesia.

Rustan Tarakka–born in Pinrang on August 27th 1975 is a Lecturer in the Department of Mechanical Engineering, Faculty of Engineering, Hasanuddin University, Makassar, Indonesia. He holds a doctoral degree from University of Indonesia, Jakarta, Indonesia. His research areas are on fluid dynamics and computational fluid dynamics. Dr. Rustan is a member of the Institutions of Engineers Indonesia.

Jalaluddin–born in Sompu on August 25th 1972 obtained a Doctor of Engineering in Mechanical Engineering in 2012 from Saga University Japan. He is an Associate Professor of Mechanical Engineering of Hasanuddin University, Makassar, Indonesia. His area of research covers ground heat exchanger for space conditioning system, renewable energy focusing on solar energy including solar water heating system and photovoltaic applications. Dr. Jalaluddin is a member of Institutions of Engineers Indonesia.

Muh. Setiawan Sukardin –born in Makassar on May 28th1976 is a PhD student at the Department of Mechanical Engineering, Faculty of Engineering, Hasanuddin University, Makassar, Indonesia. He holds a Master degree from the Department of Mechanical Engineering, Faculty of Engineering, Hasanuddin University, Makassar, Indonesia. His research areas are on fluid dynamics and computational fluid dynamics. Setiawan is a member of the Institutions of Engineers Indonesia.

Computational and Experimental Investigations of The Efficacy of Dimple Ratios to Characteristics of Flow on Van Vehicle Models

M Setiawan Sukardin
Department of Mechanical Engineering, Hasanuddin University, Gowa, Indonesia,
Politeknik ATI Makassar, Indonesia
Email: setiawan_mkz@yahoo.co.id

Nasaruddin Salam, Rustan Tarakka, Jalaluddin
Department of Mechanical Engineering, Hasanuddin University, Gowa, Indonesia
Email: nassalam.unhas@yahoo.co.id, rustan_tarakka@yahoo.com, jalaluddin_had@yahoo.com

Muhammad Ihsan
Baramuli College of Engineering, Pinrang, Indonesia
Email: m.ihsan@stt-baramuli.ac.id

Abstract: ***One of the most critical challenges facing automotive engineers worldwide is to present vehicles with the lowest aerodynamic drag. The method that can be applied to delay separation and to reduce longitudinal wake and vortex formation is passive control, in the form of dimples in the separation area. The research objective focuses on reducing aerodynamic resistance through the analysis of flow pattern characteristics and pressure fields. The test model used is the Reverse Ahmed body, which has a 1:6 ratio to the real Ahmed model. For the flow and pressure field characteristics, the data were obtained through a computational approach. The computational result of aerodynamic resistance was validated by experimental testing. Passive control is applied in 1 line dimple configuration and two zigzag lines with dimple ratios of 0.20, 0.25, and 0.50. The results showed that dimples in the vehicle model reduced longitudinal wake and vortex formation by delaying flow separation, increasing pressure efficiency, and reducing the highest aerodynamic drag by 12.092% for the computational and 8.923% for the experimental approach.***

Index term: ***Van Vehicle, Passive Control, Dimple Ratio, Pressure Distribution, Drag Aerodynamics***

I. Introduction

The challenge facing automotive scientists worldwide is to present a vehicle with the lowest aerodynamic drag. It is related to efforts to save fuel consumption and environmental aspect. Previous research has proven that a 15% reduction in aerodynamic drag can give fuel consumption savings of 5–7% [1].

The vehicle's aerodynamic drag consists of 2 main components; frictional drag, contributing to 20% of total drag [2], and pressure drag, contributing other 80% [3]. These two components are closely related to the characteristics of the flow patterns and the pressure field that occurs on the vehicle's rear wall. When the fluid reaches the top of the vehicle's rear, the flow will lose momentum to move along vehicle's rear parts. As a result, the flow will undergo a separation process and create a backflow, which causes negative pressure on the back wall and triggers backward suction. It will create a pressure difference between the front and rear sides, which is the leading cause of aerodynamic drag that works [4,5]. Apart from flow separation, aerodynamic drag is also caused by a longitudinal vortex on the rear wall. A proportion of the flow that loses momentum to move along with the body shape will be pushed sideward due to differences of flow velocities in mid parts of vehicles. This difference in velocity is a significant factor in the emergence of longitudinal vortices [6]. An in-depth evaluation of the vortex structure that forms around the vehicle body is essential to ensure vehicle stability while driving [7]. Therefore, efforts to reduce the aerodynamic drag acting on the vehicle can be made by delaying flow separation and minimizing vortex formation intensity.

One method that can be applied is passive control at the starting point of the separation process. The application of passive controls is considered more efficient because it does not involve additional energy and tends to be more applicable because it does not require significant modifications to the vehicle body. One of the passive controls that need to be considered to be implemented is a dimple.

Chear and Dol examined the effect of dimple application on Ahmed body on aerodynamic drag through a numerical computational approach with a k-epsilon turbulence model and an upstream velocity of 40 m/s. The dimple ratios used were 0.05, 0.2, 0.3, 0.4, and 0.5, respectively. The results showed a delay in flow separation and the highest reduction in aerodynamic drag obtained at the dimple ratio, DR = 0.4 of 1.95% [8].

Wong and Dol studied the effect of dimple application on simplified vehicle models through a computational simulation approach with the k-epsilon turbulence model at Reynolds number 176,387. The dimple ratios applied were DR=0.05, DR=0.2, DR=0.3, DR=0.4, and DR=0.5. The results showed that dimple geometry could change the kinematics and dynamics of the flow. The maximum turbulent kinetic energy is obtained at DR=0.4, and there is a reduction in aerodynamic resistance compared to the model without the application of dimple [9]. Salam et al. have investigated of characteristics of the flow drag across dimpled square cylinders, computational and experimentally, and have found out that parallel configurations gave higher reduction than the one that zigzag configurations could produce [10]. Sukardin et al. previously studied the distribution of flow through inline dimpled plate and found out that more dimple rows tend to produce more pressure coefficient decreases [11]. Based on the description above, studies on passive control to reduce drag aerodynamics in the form of dimple ratio variations are still limited to certain models. Meanwhile, the van model represented in the Ahmed body reversed model has not been further investigated. The aim of the research is to find the characteristic of the aerodynamics drag on the reverse Ahmed body at various dimple ratios.

II. METHODOLOGY

The test model used is a Reverse Ahmed Body, a modification of the original Ahmed model by changing the flow direction. The designed vehicle has been researched to analyze its flow dynamic [12, 13, 14]. The test model's dimension comparison against the original Ahmed model is 0.17 (1:6). The dimensions are written, length, l=174 mm, height, h=48 mm, and width, w=64.83 mm. The slope of the front geometry is determined to be 25°. Passive control in the form of dimples is placed on the upper side of the vehicle model's rear, which is believed to be the starting location for the flow separation process. This research applies dimple configurations of 1 line and 2-zigzag lines with the dimple ratio of each configuration DR=0.20, DR=0.25, and DR=0.50. The upstream velocity used is 22.2 m/s. Details of the test model are shown in Figure 1.

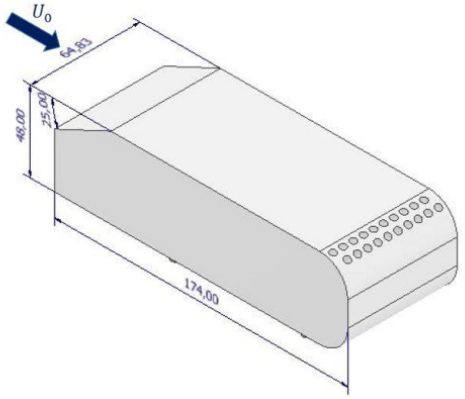

Figure 1 Test model

The research is focused on the analysis of aerodynamic resistance through computational and experimental approaches that are supported by displaying the characteristics of the flow pattern in the form of velocity pathlines and pressure fields on the rear wall of the vehicle model obtained through a computational approach.

Based on various studies, it has been revealed that 80% of the total resistance is caused by low pressure on the rear wall of the vehicle [15]. It is the main reason why the pressure field data collection is determined on the vehicle model's rear wall. For the axes along the model's width, the pressure data are obtained for five grid rows. The ratio of the width of the grid to the width of the rear wall of the vehicle model is written z/w=-1/2, z/w =-1/4, z/w=0, z/w=1/4, and z/w=1/2. The ratios of the grid height to

the model height (y/h) are 0.17, 0.33, 0.50, 0.67, and 0.83, respectively, as shown in Figure 2.

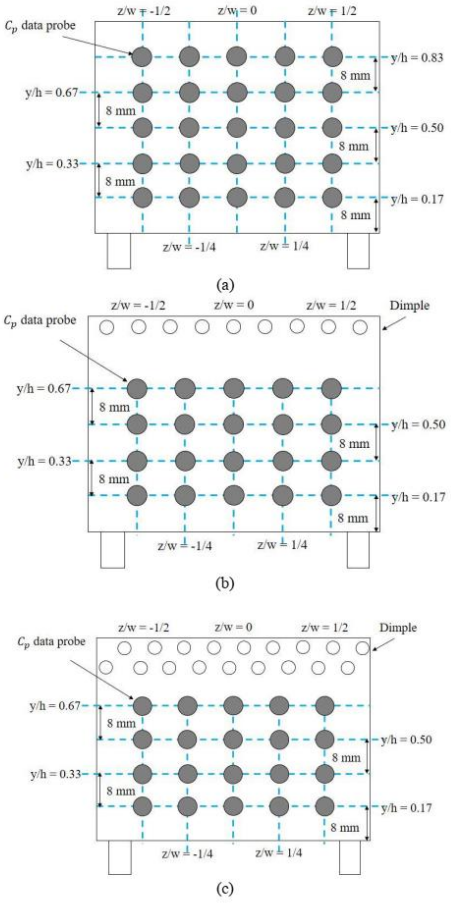

Figure 2 Location of pressure field data collection: (a) Without control, (b) With 1-line dimple, (c) With 2-zigzag dimple lines.

The ratios of the grid height to the model height (y/h) are 0.17, 0.33, 0.50, 0.67, and 0.83, respectively. The pressure value obtained is written in a dimensionless number, the pressure coefficient (Cp), defined in equation 1 [16]:

$$C_p = \frac{P - P_0}{\frac{1}{2}\rho U^2} \qquad (1)$$

After the design process, the vehicle model is then defined into the computational domain, as shown in Figure 3. Hence, the meshing process and defining boundary conditions on the Gambit device, as shown in Figure 4, take parts. Furthermore, the model will go through an iteration process using fluent software tools. The computational conditions are shown in table 1.

TABLE 1: COMPUTATIONAL CONDITION

Fluid	Air	-
Fluid properties	Density	1.225 kg/m^3
	Viscosity	1.7894 × 10^{-5} kg/m.s
Boundary conditions	Model	Wall
	Outlet	Pressure outlet
	Inlet	Velocity inlet
	Wall	Wall
Upstream velocity (U_0)		22.2 m/s
Reverse Ahmed body 1:6	1-line dimple	DR=0.20
	2-zigzag lines	DR=0.25
		DR=0.50

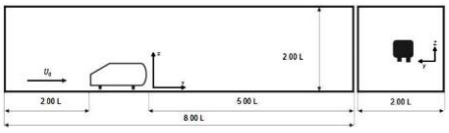

Figure 3 Computational domain

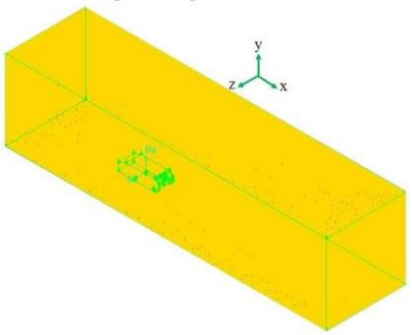

Figure 4 Mesh display.

Figure 5, Hence, The experimental measurement of aerodynamic drag utilizes a load cell device placed around the subsonic wind tunnel. The model is placed in the section via an aluminium support rod connected to the load cell. Drag data is automatically displayed on a computer connected to an Arduino Uno device. Data retrieval duration was determined to be 2 minutes for each model, both without dimple and for models with the application of 1 line and two zigzag dimple passive control, and we get 120 data for each model. The 120 data are averaged and

written into dimensionless units using equation 2 [17] to be compared with the results obtained through a computational approach.

$$C_d = \frac{F_d}{\frac{1}{2}\rho U^2 A} \qquad (2)$$

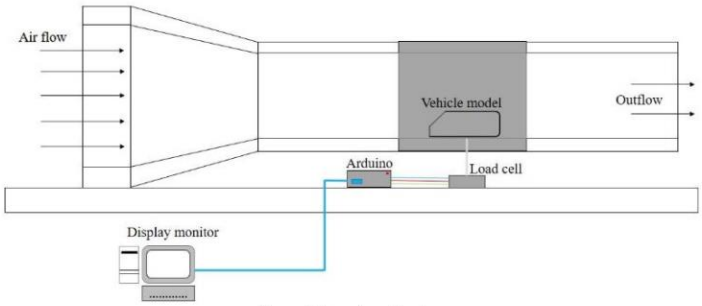

Figure 5 Experimental setup

III. Results And Discussion

A. *The Flow Patten Characteristic*

The flow pattern characteristics comparison of the model without passive control and the model with the application of passive controls in the form of dimples is shown in Figures 6, 7, and 8. For models without passive control, it shows a relatively large wake formation due to the separation process that occurs right on the vehicle model's rear wall. The separation occurs fast enough, causing the fluid flow to lose momentum to move along the shape of the belted body. Apart from forming a backflow right against the back wall, it is also pushed sideward due to the significant differences of flow velocities between the center and sides. This difference in velocity is the main trigger for the appearance of the longitudinal vortex phenomenon.

Models with the application of passive control in the form of dimples have shown delays in flow separation. The separation process tends to move away from the back wall, resulting in backflow formation far away from the rear wall. The longitudinal vortex was also reduced for all models. Visually, it can be seen that the most considerable reduction in longitudinal vortex intensity occurs in the model with the application of zigzag dimple configuration at DR=0.50. For this model, the flow line formed on the rear side tends to be straighter and at the same time has a smaller wake formation structure compared to other models. These results are consistent with Chear and Dol's findings, which revealed that the application of passive control in the form of dimples could delay flow separation and reduce wake formation [8].

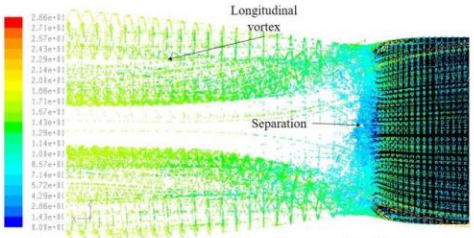

Figure 6 Flow pattern characteristics of each model without dimples

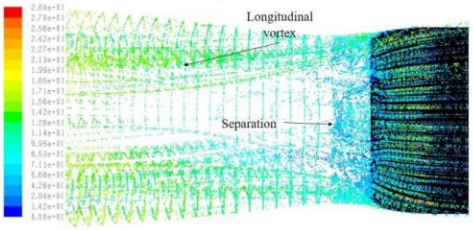

(a) With 1-line dimple, DR=0.20

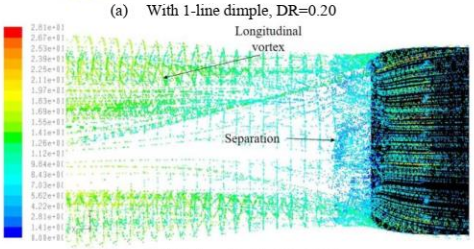

(b) With 1-line dimple, DR=0.25

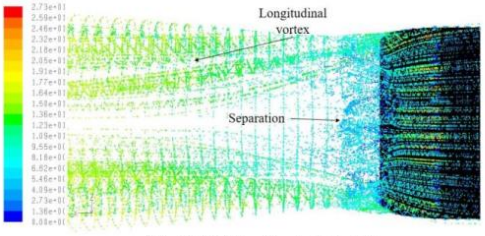

(c) With 1-line dimple, DR=0.25

Fig. 7. Flow pattern characteristics of each model 1-line dimple

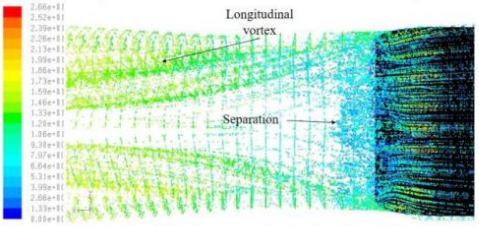

(a) With 2-zigzag dimple lines, DR=0.20

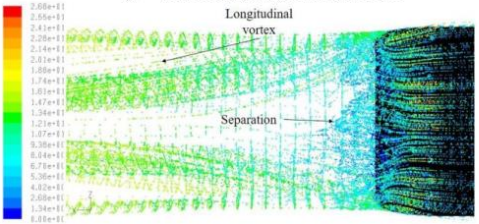

(b) With 2-zigzag dimple lines, DR=0.25

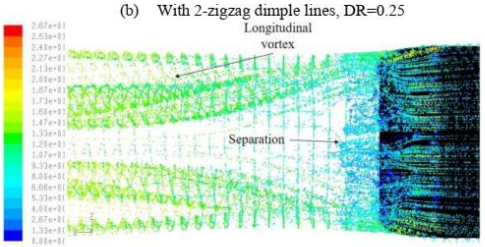

(c) With 2-zigzag dimple lines, DR=0.50

Fig. 8. Flow pattern characteristics of each model 2-zigzag dimple lines

B. Pressure Field

The comparison of the minimum pressure coefficient of the model without dimple and the model with the application of dimple configuration of one line and two zigzag lines in each dimple ratio, DR=0.20, DR=0.25, and DR=0.50 is shown in Table 2. The lowest average minimum pressure coefficient (Cp) of -0.456 has been obtained in the model without control. The minimum pressure coefficient has been obtained at the ratio of the grid height to the model height (y/h) of 0.83. It is because this position is where the flow separation process starts. These findings confirm the flow pattern characteristics shown in Figure 6, where the no-dimple model is the model with the most extensive longitudinal wake and vortex formation compared to other models. This result is correlated with Anderson's findings, which reveal that the pressure field tends to be low in the area where the flow separation occurs [18].

Models with the application of 1 line dimple at DR 0.20, 0.25, and 0.50 respectively, have shown increases in the average minimum pressure coefficient compared to those on the model without the dimples. The increases are sequentially at 15.607%, 16.002%, and 19,903%, where the minimum pressure coefficients on the average of each dimple ratio are at -0.385 for DR=0.20, -0.383 for DR=0.25, and -0.365 for DR=0.50. The model with the application of the two zigzag line dimples also shows a significant increase in pressure efficiency. The increases in average minimum pressure for each dimple ratio have been recorded at 21.623% for DR=0.20, at 21.579% for DR=0.25, and at 22.665% for DR=0.50, whereas the average minimum pressure coefficients have been recorded respectively -0.357, -0.358, and -0.353.

Overall, it was found that the application of passive control in the form of 1 line dimple and zigzag configurations at the respective DR ratios of 0.20, 0.25, and 0.50 on the upper side of the rear of the vehicle model was able to increase the average minimum swallow coefficient. The highest minimum pressure coefficient increase is obtained in a model with a two zigzag line dimple configuration at DR=0.50 of 22.665%. This result correlates with the velocity pathlines shown in Figure 8 (c), which shows that the model with dimple zigzag configuration at DR=0.50 has the smallest wake and longitudinal vortex formation compared to other models.

TABLE 2: THE MINIMUM PRESSURE COEFFICIENT OF EACH MODEL

z/w	Pressure coefficient (C_p)						
	Without dimple	1 line dimples			2-zigzag lines dimples		
		Dimple Ratio (DR)					
		0.20	0.25	0.50	0.20	0.25	0.50
-1/2	-0.399	-0.392	-0.397	-0.338	-0.303	-0.312	-0.309
-1/4	-0.431	-0.348	-0.351	-0.347	-0.357	-0.332	-0.309
0	-0.526	-0.418	-0.423	-0.424	-0.412	-0.418	-0.391
1/4	-0.431	-0.368	-0.351	-0.347	-0.330	-0.332	-0.364
1/2	-0.494	-0.399	-0.394	-0.371	-0.385	-0.394	-0.391
Average	-0.456	-0.385	-0.383	-0.365	-0.357	-0.358	-0.353
Enhancement (%)	-	15.607	16.002	19.903	21.623	21.579	22.665

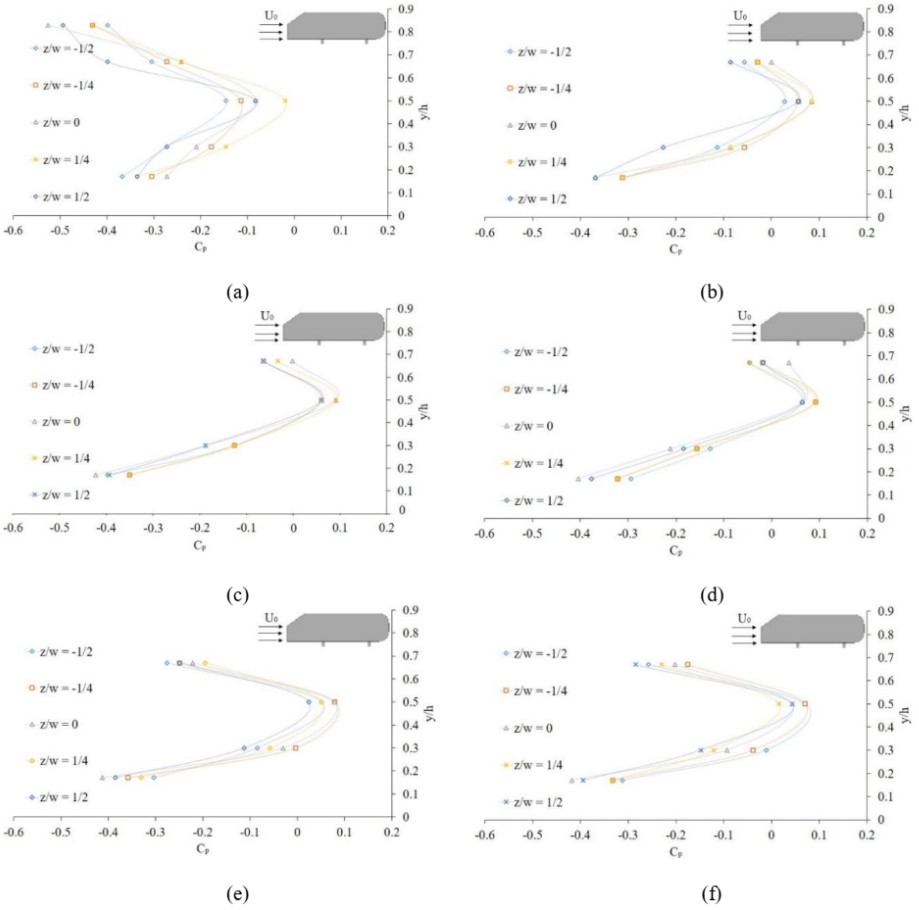

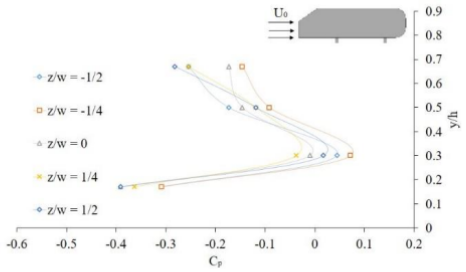

(g)

Fig. 9. Comparison of the minimum pressure coefficient for each model: (a) Without Dimples, (b) With 1 line dimples, DR=0.20, (c) With 1 line dimples, DR=0.25, (d) With 1 line dimples, DR=0.50, (e) With 2-zigzaglines dimples, DR=0.20, (f) With 2-zigzag lines dimples, DR=0.25, (g) With 2-zigzaglines dimples, DR=0.50.

C. Aerodynamics Drag

Table 3 shows the drag coefficient's values from the numerical computation of the model without dimple and the model with the application of 1-line and two zigzag lines on DR 0.20, 0.25, and 0.50. The highest drag coefficient of 1.439 has been obtained in the model without control. For 1-line dimple model, the drag coefficients for each DR have been recorded at 1.310 for DR=0.20, at 1.302 for DR=0.25, and at 1.293 for DR=0.50. Whereas for a model with two zigzag lines dimple, the drag coefficients of DR 0.20, 0.25, and 0.50 are written as 1.273, 1.279, and 1.265, respectively.

TABLE 3: CD COMPUTATIONAL APPROACH

Model	DR	C_d
Without dimple	-	1.439
With 1 lines dimple	0.20	1.310
	0.25	1.302
	0.50	1.293
With 2-zigzag lines dimple	0.20	1.273
	0.25	1.279
	0.50	1.265

In agreement to the computational approach, the experimental approach also shows that the highest drag coefficient has been obtained in the no-dimple model, at the value of 1.300. For a model with 1-line dimple application, the drag coefficients of each dimple ratio have been recorded at 1.218 for DR=0.20, at 1.207 for DR=0.25, and at 1.192 for DR=0.50. For the model with the application of 2-zigzag dimples configuration, the drag coefficient of the DR 0.20, 0.25, and 0.50 dimple ratios are recorded at 1.185, 1.187, and 1.184, respectively.

TABLE 4: CD EXPERIMENTAL APPROACH

Model	DR	C_d
Without dimples	-	1.300
With 1 lines dimple	0.20	1.218
	0.25	1.207
	0.50	1.192
With 2-zigzag lines dimple	0.20	1.185
	0.25	1.187
	0.50	1.184

A comparison of the aerodynamic drag reduction with computational and experimental approaches is shown in Table 5. For models with the 1-line dimples, the reduction is increased along as dimple ratios enlarge both computationally and experimentally, as shown in Figure 10. For models with 2-zigzag lines configuration, the percentages of the increase in a drag reduction fluctuate both computationally and experimentally. The highest decrease was obtained as well at DR=0.50.

Overall, it shows that dimples on the upper rear part of the vehicle model can reduce the aerodynamic drag of the vehicle model. The highest reduction was obtained in a model with the dimples configuration of 2-zigzag lines at DR=0.50, both computationally and experimentally. The reduction is 12.092% for the computational approach and is 8.923% for the experimental method, where the difference in reduction is 3.169%. These results are consistent with what Chear and Dol revealed that the application of dimples in vehicles could reduce aerodynamic drag while increasing fuel consumption efficiency [8].

TABLE 5: C_p REDUCTION COMPUTATIONAL AND EXPERIMENTAL METHODS

Method	Reduction (%)					
	1 line, DR			2-zigzag lines, DR		
	0.20	0.25	0.50	0.20	0.25	0.50
Computational	8.964	9.520	10.146	11.536	11.119	12.092
Experimental	6.308	7.154	8.308	8.846	8.692	8.923
Difference (%)	2.657	2.367	1.838	2.689	2.426	3.169

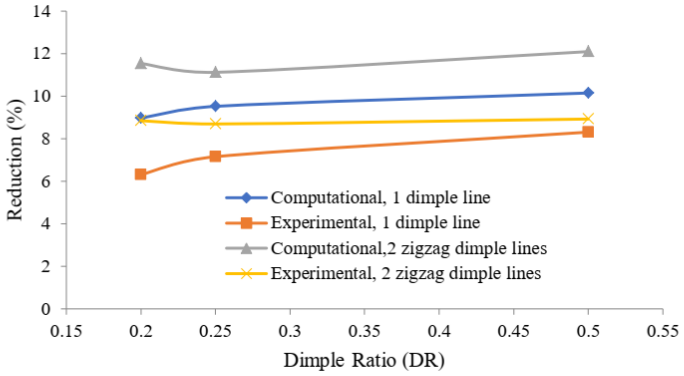

Fig. 10. Reduction comparison

IV. CONCLUSIONS

The application of passive control in the form of dimples on the upper side of the rear of the vehicle model provides significant changes to the characteristics of the flow pattern, the pressure field on the rear wall and aerodynamic drag compared to the model without the dimples. The most significant change was obtained in the model with the application of 2-zigzag lines dimples at DR=0.50, where longitudinal wake and vortex formation was significantly reduced. An average minimum pressure efficiency increase was 22.665%, and the highest aerodynamic drag reduction was 12.092% for computation and 8.923% for the experimental approach.

CONFLICT OF INTEREST

The authors declare no conflict of interest.

AUTHOR CONTRIBUTIONS

Mr. MS. Sukardin, main author, conducted CFD and experimental research, wrote the manuscript. Dr. N. Salam organized research promotion, supervised research. Dr. R. Tarakka, corresponding author, conducted research planning, Dr. Jalaluddin, conducted research, and Mr. M. Ihsan, wrote and translated the manuscript. All authors had approved the final version.

ACKNOWLEDGMENTS

We gratefully thanks the Head of The Agency of Industrial Human Resource Development (Badan Pengembangan Sumber Daya Manusia Industri-BPSDMI), The Ministry of Industry, The Republic of Indonesia for the research funding. We also gratefully thanks the Head of Fluid Mechanics Laboratory of Hasanuddin University who has facilitated the data collection process.

REFERENCES

[1] Bellman M, Agarwal R, Naber J, Chusak L. *Reducing energy consumption of ground vehicles by active flow control*, Energy Sustainability, 43949: 785–93, (2010).

[2] Wood RM, *Impact of advanced aerodynamic technology on transportation energy consumption*, SAE transactions, 854–74, (2004)

[3] Sudin MN, Abdullah MA, Shamsuddin SA, Ramli FR, Tahir MM. *Review of research on vehicles aerodynamic drag reduction methods*, International Journal of Mechanical and Mechatronics Engineering. 14: 37–47, (2014).

[4] Hilleman TB, *Vehicle drag reduction with air scoop vortex impeller and trailing edge surface texture treatment*, US Patent No. US 7,192,077 B1, (2007).

[5] Barros D, Borée J, Noack B, Spohn A, Ruiz T, *Effects of Unsteady Coanda Blowing on the Wake and Drag of a Simplified Blunt Vehicle In: Pollard A., Castillo L., Danaila L., Glauser M. (eds) Whither Turbulence and Big Data in the 21st Century*, Springer, Cham. https://doi.org/10.1007/978-3-319-41217-7_19 , (2017).

[6] Harinaldi, Budiarso, Tarakka R, Simanungkalit SP, *Effect Active control by blowing to aerodynamic drag of bluff body van model*, International Journal of Fluid Mechanics Research. Vol. 40 No. 4, pp. 312-323, (2013).

[7] Nakashima T, Tsubokura M, Nouzawa T, Nakamura T, Zhang H, Oshima N, *Large-eddy simulation of unsteady vehicle aerodynamics and flow structures*, BBAA VI International Colloquium on: Bluff Bodies Aerodynamics & Applications (Citeseer): 1–14, (2008).

[8] Chear C, Dol S, *Vehicle aerodynamics: drag reduction by surface dimples,* International Journal of Mechanical and Mechatronics Engineering. 9: 202–5, (2015).

[9] Wong S, Dol S, *Simulation Study on Vehicle Drag Reduction by Surface Dimples,* International Journal of Mechanical and Mechatronics Engineering. 10(3): 560–565, (2016).

[10] Salam, N., Tarakka, R., Jalaluddin, Ihsan, M., *Computational and experimental studies of characteristics of the flow drag, through dimpled square cylinders,* International Journal of Mechanical and Production Engineering Research and Development, 2019, 9(6), pp. 677-690, DOI: 10.24247/ijmperddec201958, (2019).

[11] Sukardin, M.S., Salam, N., Tarakka, R., Jalaluddin, Ihsan, M, Computational studies of pressure distribution of flow through inline dimpled plate. IOP Conference Series: Materials Science and Engineering, 885(1), 012022. DOI: 10.1088/1757-899x/885/1/012022, (2020).

[12] Rauf W, Tarakka R, Jalaluddin, Ihsan M., *Effect of Flow Separation Control with Suction Velocity Variation: Study of Flow Characteristics, Pressure Coefficient, and Drag Coefficient*, Universal Journal of Mechanical Engineering 8(3): 142-151. DOI: 10.13189/ujme.2020.080302, (2020).

[13] Tarakka R, Jalaluddin, Mire B, Umar MN., *Effect of Turbulence Model In Computational Analysis of Active Flow Control on Aerodynamic Drag of Bluff Body Van Model*, International Journal of Applied Engineering Research, 10(1): 207-219, (2015).

[14] Tarakka R, Salam N, Jalaluddin, Ihsan M., *Effect of Blowing Flow Control and Front Geometry Towards the Reduction of Aerodynamic Drag on Vehicle Models*, FME Transactions.47(3): 552-559. DOI: 10.5937/fmet1903552T, (2019).

[15] Kourta A, Gilliéron P., *Impact of the automotive aerodynamic control on the economic issues*, Journal of Applied Fluid Mechanics. 2(2): 69–75, (2009).

[16] Cengel YA, Cimbala JM, *Fluid Mechanics: Fundamental and Applications*, Third edition, Mc Graw Hill, ISBN 978-0-07-338032-2, (2014).

[17] Munson BR, Okiishi TH, Huebsch WW, Rothmayer AP, *Fundamentals of Fluid Mechanics*, John Wiley & Sons, Inc., (2013).

[18] Anderson JD, *Fundamental of Aerodynamics*. McGraw-Hill Series in Aeronautical and Aerospace Engineering. University of Mayland. Third edition. ISBN 0-07237335-0, (2001).

Muh. Setiawan Sukardin –born in Makassar on May 28th 1976 is a PhD student at the Mechanical Engineering Department, Hasanuddin University, Indonesia. He holds a Master degree from the Department of Mechanical Engineering, Faculty of Engineering, Hasanuddin University, Makassar, Indonesia. His research areas are on fluid dynamics.

Nasaruddin Salam – born in Bulukumba on December 20th 1959 is a Professor and the Chairman of Fluid Mechanics Laboratory in Mechanical Engineering Department, Hasanuddin University, Indonesia. He has a doctoral degree from Brawijaya University, Malang Indonesia. His research includes fluid dynamics.

Rustan Tarakka–born in Pinrang on August 27th 1975 is an Associate Professor in Mechanical Engineering Department, Hasanuddin University, Indonesia. He has a doctoral degree from University of Indonesia, Jakarta, Indonesia. His research areas are on fluid dynamics.

Jalaluddin – born in Sompu on August 25th 1972 obtained a Doctor of Engineering in Mechanical Engineering in 2012 from Saga University Japan. He is an Associate Professor, in Mechanical Engineering Department, Hasanuddin University, Indonesia. His area of research covers fluid mechanics and heat transfers.

Muhammad Ihsan -born in Watampone, February 20th 1977, is a lecturer on Baramuli College of Engineering, Indonesia. He graduated with a bachelor degree and a professional degree in engineering from Hasanuddin University and masters in transport engineering from Asian Institute of Technology, Bangkok, Thailand and Universitas Gajah Mada, Yogyakarta, Indonesia. His research includes transport engineering, fluid mechanics and hydraulics.